High wintertime particulate matter pollution over an offshore island (Kinmen) off southeastern China: An overview

S. C. Hsu,[1] S. C. Liu,[1] F. Tsai,[2] G. Engling,[1,3] I. I. Lin,[4] C. K. C. Chou,[1] S. J. Kao,[1] S. C. C. Lung,[1,4] C. Y. Chan,[5] S. C. Lin,[6] J. C. Huang,[7] K. H. Chi,[1] W. N. Chen,[1] F. J. Lin,[8] C. H. Huang,[1] C. L. Kuo,[1] T. C. Wu,[1] and Y. T. Huang[1,8]

Received 1 December 2009; revised 17 May 2010; accepted 26 May 2010; published 15 September 2010.

[1] Both the Yangtze River Delta (YRD) and the Pearl River Delta (PRD), the two most rapidly developing areas in eastern China, have suffered from serious air pollution, and thus, numerous investigations were devoted to studying these problems. Other areas in eastern China have received less attention despite similar rapid development in their industries and economy. In this study, we analyzed air-quality data from Kinmen Island (24°27′26″N, 118°19′36″E) located off Fujian Province and between the two above-mentioned deltas. Our results clearly show that the study area is experiencing serious air quality deterioration. Particularly, high levels of suspended particulate matter (PM) were observed during winter, when the northeasterly monsoon prevails. For example, concentrations of wintertime PM_{10} (particles ≤ 10 μm in diameter) frequently exceeded 100 $\mu g/m^3$ in the last three years. In addition to the air-quality data analysis, aerosol samples were collected between 22 November 2007 and 6 March 2008 and subjected to chemical analyses of various species. Our findings show that the three principal PM components include organic, mineral, and sulfate species with moderate to minor fractions of nitrate, sea salt, elemental carbon, and trace metal oxides. The high PM levels observed over the island may be partly attributed to the transport from a mixed-type industrial area located ~40 km northeast of Kinmen. Our study could partially fill the air quality data gap between the YRD and PRD regions, and highlight the alarming fact that air pollution has gradually expanded along eastern China's coastal zone.

Citation: Hsu, S. C., et al. (2010), High wintertime particulate matter pollution over an offshore island (Kinmen) off southeastern China: An overview, *J. Geophys. Res.*, *115*, D17309, doi:10.1029/2009JD013641.

1. Introduction

[2] Aerosol particles are composed of a complex mixture of various chemical components, such as sulfate, nitrate, and ammonium salts, mineral dust, sea salt, and carbonaceous species [*Andreae and Crutzen*, 1997]. These particles have significant adverse affects on visibility deterioration, public health, the environment, ecology, climate, and biogeochemistry [*Seinfeld*, 1989; *Andreae and Crutzen*, 1997; *Prather et al.*, 2008]. For instance, airborne dust causes radiative forcing [*Tegen et al.*, 1996], although it has large uncertainties in terms of the magnitude and direction (positive or negative) of the forcing due to the irregular shape of dust particles and modified physicochemical properties during transport [*Intergovernmental Panel on Climate Change*, 2001; *Kahnert et al.*, 2005]. Dust associated with iron has been confirmed to contribute essential micronutrients, such as iron, to the oceans, stimulating primary production [*Martin et al.*, 1994], which is likely linked to carbon sequestration [*Cooper et al.*, 1996]. Carbonaceous aerosols have been demonstrated to enhance global warming, as they have strong capabilities for radiation forcing [*Seinfeld*, 2008]. Sulfate aerosol particles serve as the most important cloud condensation nuclei, therefore affecting climate change via the indirect radiative aerosol effect [*Charlson et al.*, 1992]. Chemical toxins, such as heavy metals and persistent organic particulates, associated with inhalable particles (≤ 10 μm in diameter, also referred to as PM_{10}), are harmful to human health [*Ondov et al.*, 2006; *Yauk et al.*, 2008; *Wei et al.*, 2009]. For example, *Finkelman et al.* [1999] drew attention to aerosol fluorides, mainly

[1]Research Center for Environmental Changes, Academia Sinica, Taipei, Taiwan.
[2]Department of Marine Environmental Informatics, National Taiwan Ocean University, Keelung, Taiwan.
[3]Department of Biomedical Engineering and Environmental Sciences, National Tsing Hua University, Hsinchu, Taiwan.
[4]Department of Atmospheric Science, National Taiwan University, Taipei, Taiwan.
[5]School of Environmental Science and Engineering, Sun Yat-Sen University, Guangzhou, China.
[6]Department of Construction Engineering, National Quemoy University, Kinmen, Taiwan.
[7]Department of Geography, National Taiwan University, Taipei, Taiwan.
[8]Institute of Oceanography, National Taiwan University, Taipei, Taiwan.

0148-0227/10/2009JD013641

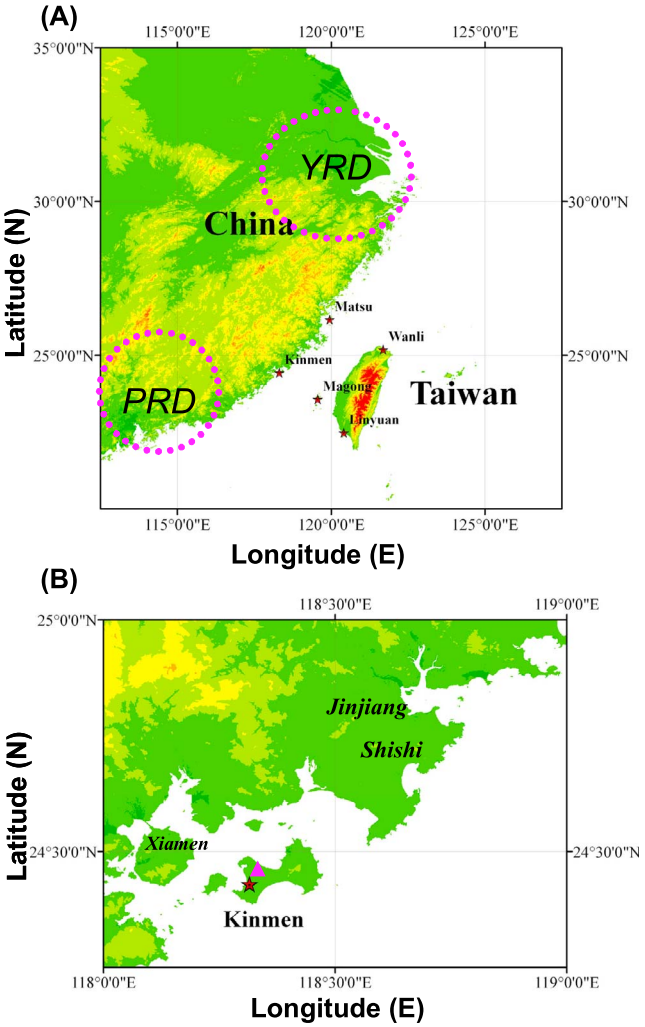

Figure 1. Location maps. (a) A regional map showing the relative location of Kinmen Island off Fujian Province, southeastern China, between the Yangtze River Delta (YRD) in northern China and the Pearl River Delta (PRD) in southern China. Also shown are five Taiwan EPA air quality stations (red stars): Kinmen and Matsu, two offshore island stations of southeastern Fujian Province; Linyuan, an industrial station close to the Linyuan Petrochemical Park, southern Taiwan; Wanli, a background station at the northern tip of Taiwan; and Magong, an offshore island background station on the Penghu Islands in the Taiwan Strait. (b) A local map showing the aerosol sampling station on Kinmen Island (pink triangle; 24°27′26″N, 118°19′36″E) operated for this study. An air-quality monitoring station (red star) maintained by Taiwan's EPA is ~3 km south of our sampling site. Jingjiang City and Shishi City are located 40–50 km northeast of Kinmen Island. These are the two areas suggested to most likely be the source of air pollutants deteriorating Kinmen air quality (see text for more information).

originating from coal combustion, which may induce dental and skeletal fluorosis.

[3] It has been well documented that both the Yangtze River Delta (YRD) in northern China and the Pearl River Delta (PRD) in southern China are suffering from severe air pollution in terms of their PM and ozone levels [*Chan and Yao*, 2008]. Accordingly, numerous field investigations have been devoted to determining the characteristics and formation mechanisms of pollution in these regions, and pollution control and management strategies have been implemented by governmental agencies. In the recent decade, the remaining coastal zones in eastern China (aside from the two deltas mentioned above) have also experienced accelerated economic growth with the expansion of low-end industrial and manufacturing operations. As demonstrated from satellite images, spatial distribution of aerosol optical thickness (AOT) over eastern China has clearly been associated with a zonal increase in air pollution [*Chu et al.*, 2003; *Guo et al.*, 2009]. Unfortunately, there are few observational studies on air pollution and the physicochemical characteristics of atmospheric particulates reported from this area [*Fang et al.*, 2009]. Kinmen Island is situated off Fujian Province in southeastern China. Its position is in-between the YRD and the PRD (Figure 1a), two of the most dynamic areas characterized by rapid development in industrialization and urbanization in China. Thus, Kinmen Island may be subject to substantial influence of air pollutant emissions from the YRD and PRD following long-range transport (LRT), aside from local source contributions, depending on the meteorological and synoptic atmospheric conditions. Kinmen Island could, therefore, be a key location for comprehensive investigations of the relevant issues related to regional air pollution, partly filling an important data gap.

[4] Few studies on atmospheric particles, as well as other air pollutants, have been reported for Fujian Province. Moreover, any study performed in this region was conducted for short time periods and focused on only a few chemical species, such as polycyclic aromatic hydrocarbons (PAHs) [*Hong et al.*, 2007; *Wang et al.*, 2007]. *Hong et al.* [2007], however, concluded that the PAH pollution was not serious in Xiamen, another island off the southeastern Fujian Province, around 8 km west of Kinmen (Figure 1b).

[5] In this study, we analyzed air-quality data for PM (PM_{10} and $PM_{2.5}$), sulfur dioxide (SO_2), nitrogen oxides (NO_x) (including nitrogen dioxide (NO_2) and nitric oxide (NO)), and carbon monoxide (CO) on Kinmen Island, collected by the Environmental Protection Administration (EPA) of Taiwan (Republic of China), with an emphasis on PM. More importantly, we give an overview of various chemical components of aerosol particles collected during the winter season between late November 2007 and early March 2008, a comparably polluted season in the study area. On the basis of the present data set of aerosol chemistry, we discuss regional air pollution in terms of its chemical characteristics, source contributions, and implications on various environmental processes.

2. A Brief Background of the Study Location

[6] Kinmen Island is located off Fujian Province, China (Figure 1a). It comprises an area of 132 km^2 and has a population of about 57,000. Kinmen's annual mean temperature is 20.9°C, with a maximum in August and minimum in January. Average annual precipitation in Kinmen is 1072 mm, concentrated between April and September, while its annual relative humidity averages 79%. Northeasterly monsoons begin approximately in mid-September, whereas

in mid- to late May southwesterly winds start to prevail. At present, tourism is the primary type of economy in Kinmen. There are few industrial activities on the island, mainly limited to two low-sulfur heavy-oil-fired thermal power plants: Ta-Shan and Xia-Xing Thermal Power Plants. The former is located 7 km southwest of our aerosol sampling site and 4 km from EPA's Kinmen air-quality monitoring station. The latter is 7.5 km southeast of our sampling site and 8.8 km from the EPA air-quality station. The energy output of the two power plants is 64.6 and 20.3 MW, respectively. The impact of these local emission sources on the Kinmen PM levels may be insignificant, particularly during the northeasterly monsoon season, as the power plants are located downwind of most of the island's land area, including the two monitoring stations.

3. Materials and Methods

3.1. Air-Quality Data Acquisition

[7] Air-quality data, including those for PM, SO_2, CO, and NO_x (sum of NO_2 and NO), and meteorological parameters (temperature, relative humidity, and wind speed and direction) were obtained from an air-quality monitoring station on Kinmen (24°25′45.72″N, 118°18′55.05″E) (Figure 1b) operated by the EPA of Taiwan. The instruments used at this station included a model 43 pulsed fluorescent SO_2 analyzer (equations A-0276-009), model 48 gas filter correlation ambient CO analyzer (RFCA-0981-054), model 42 chemiluminescence NO-NO_2-NO_X Analyzer (RFNA-1289-074), and model 650 (Wedding and Associates) PM_{10} Beta gauge automated particle monitor (EQPM-0391-081). In this report we use hourly (http://taqm.epa.gov.tw/taqm/zh-tw/HourlyData.aspx) and monthly (http://taqm.epa.gov.tw/taqm/zh-tw/MonthlyAverage.aspx) data to demonstrate the severe air pollution over Kinmen Island during winter. The Kinmen EPA station was situated approximately 3 km south of our aerosol sampling station, which is described in more detail below. For comparison, monthly data were used from an industrial air-quality monitoring station (Linyuan, within 1 km of the Linyuan Petrochemical Industrial Park; 22°28′45.64″N, 120°24′42.64″E), in Kaohsiung County, Southern Taiwan (Figure 1a). In order to identify whether or not the high PM levels in Kinmen were influenced by regional LRT, mainly from northern China and the YRD, data from three additional Taiwan EPA monitoring stations were selected (Figure 1a): Wanli (25°10′46.8″N, 121°41′23.57″E) at the northern tip of Taiwan, Magong (23°34′08.51″N, 119°33′58.17″E) on Penghu Island in the Taiwan Strait, and Matsu (26°09′39.42″N, 119°56′57.75″E), another offshore island of Fujian Province approximately 250 km northeast from Kinmen.

3.2. Aerosol Sampling

[8] In this study, two types of aerosol samples were collected: dichotomous samples, including $PM_{2.5}$ (particle size less than 2.5 μm aerodynamic diameter) and $PM_{2.5–10}$ (particle size from 2.5 to 10 μm in diameter), as well as total suspended particulate (TSP) samples. The aerosol sampling station was set at Jinning Elementary and Junior High School (24°27′26″N, 118°19′36″E), located 3 km north of the Kinmen EPA air-quality monitoring station. The aerosol samplers, including a low-volume dichotomous sampler (Thermo Andersen SA241) and a high-volume (Hi-vol) TSP sampler (Tisch Environmental, Inc.), were set up on the rooftop of a two-story building (~10 m above ground level). The former collected both $PM_{2.5}$ and $PM_{2.5–10}$ aerosol samples on a daily basis and was operated at a flow rate of 16.7 L/min; the substrates used were pre-weighed PTFE membrane filters (47 mm diameter, 1 μm pore size). The latter collected TSP samples for 48 h and was operated at a mean flow rate of ~60 m^3/hr; the substrate used were pre-baked 8″ × 10″ quartz fiber filters. The sampling period extended from 22 November 2007 to 6 March 2008. The daily filter-based $PM_{2.5}$ and PM_{10} (i.e., sum of $PM_{2.5}$ and $PM_{2.5–10}$) mass concentrations, obtained via the gravimetric method, showed good linear correlations (R = 0.88 for $PM_{2.5}$ and 0.83 for PM_{10}) with the hourly average concentrations measured by the Taiwan EPA. However, the ratios of our PM mass data relative to the EPA data were only 0.65 for both $PM_{2.5}$ and PM_{10}. These differences are likely attributed to the conditioning of our samples, resulting in loss of a certain aerosol water fraction [*Lee and Hsu*, 1998]. The average ambient relative humidity was up to 70 ± 12% during the sampling period.

3.3. Sample Preparation and Chemical Analysis of Aerosol Samples

[9] The post-weighed $PM_{2.5}$ and $PM_{2.5–10}$ samples were extracted with 20 mL Milli-Q water (18.2 MΩ) for one hour. Residual membrane samples were further digested with an acid mixture (2 mL nitric acid + 2 mL hydrofluoric acid) using a microwave digestion system (MARSXpress, CEM Corporation, Matthews, NC). The aqueous extracts were analyzed for ionic species, using ion chromatography (Dionex ICS-90 for ammonium ion (NH_4^+) and ICS-1500 for sulfate (SO_4^{2-}), nitrate (NO_3^-), chloride (Cl^-), and fluoride (F^-) ions), and 22 water-soluble metals, using a quadrupole inductively coupled plasma mass spectrometer (ICP-MS; Elan 6100; Perkin Elmer, USA). The digested filter solutions were analyzed for the water-insoluble fraction of selected metals using ICP-MS. A 1.77 cm^2 punch of each TSP-laden quartz filter was used for the measurement of both organic carbon (OC) and elemental carbon (EC), using a DRI-2001 carbon analyzer, which was operated using the IMPROVE/TOR protocol [*Chow and Watson*, 2002]. Each 1/8 piece of TSP filter that had been punched for the OC and EC analysis was then further subjected to extraction with 50 mL Milli-Q water for the determination of water-soluble organic carbon (WSOC), using a total organic carbon analyzer (O.I. Analytical Model 1010). Detailed descriptions of the methods used for the chemical analyses can be found in the literature [*Hsu et al.*, 2007, 2008, 2009a].

3.4. Data Processing and Estimation of Aerosol Components

[10] In this study, we considered the spring season (first quarter) as the period from March to May, the summer season (second quarter) from June to August, etc. The concentrations of non-sea salt SO_4^{2-} ($_{nss}SO_4^{2-}$) were calculated by subtracting the concentrations of sea salt SO_4^{2-} ($_{ss}SO_4^{2-}$) from the total SO_4^{2-} concentrations. The $_{ss}SO_4^{2-}$ concentrations were estimated by multiplying Na^+ concentrations by a factor of 0.252 [*Hsu et al.*, 2007], the typical sulfate-to-sodium mass ratio in seawater.

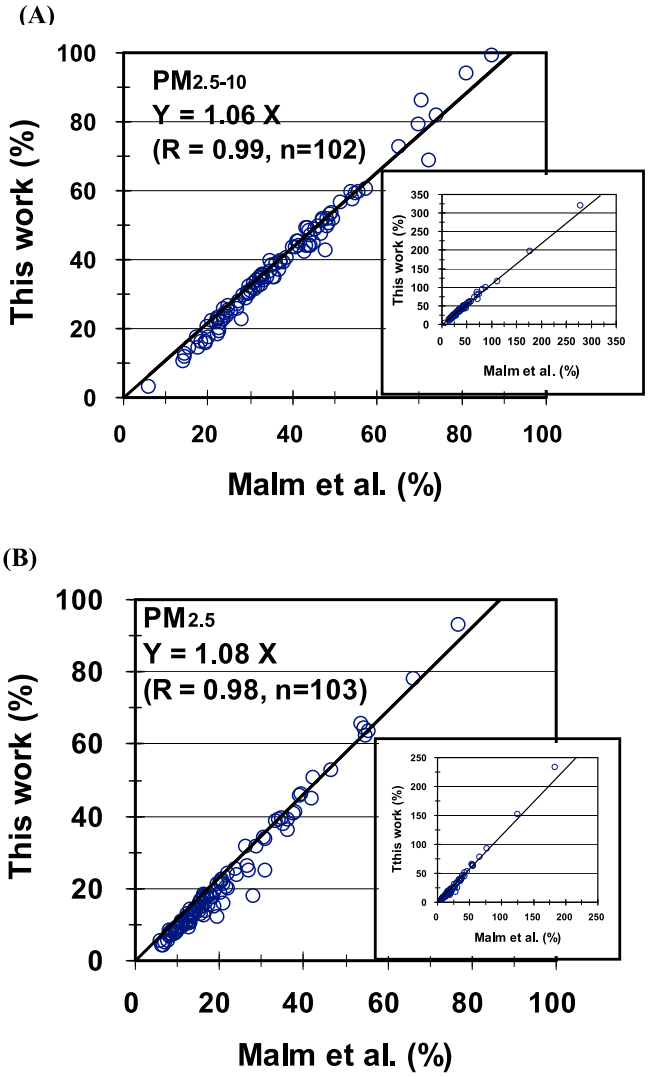

Figure 2. Scatterplots of the estimated mineral component fractions obtained by multiplying the Al concentrations by a factor of 12.5, which was adopted in this study, versus the *Malm et al.* [1994] method for (a) $PM_{2.5–10}$ and (b) $PM_{2.5}$ Kinmen aerosol particles. The insets in each plot are the plots based on all data points, whereas the enlarged plots exclude two and three outliers, respectively. Also shown in the enlarged plots are the linear regression lines (forced through the origins) and the regression equations.

[11] Note that EC and OC were measured using the Hi-vol TSP samples collected on quartz filters, different from the other chemical species that were measured from the low-volume dichotomous samples collected on PTFE membrane filters. Therefore, weight concentrations of EC and OC were calculated by dividing the quartz filter-obtained EC and OC atmospheric concentrations by the PTFE-obtained PM mass concentrations, assuming that EC and OC are mostly associated with PM_{10} aerosol particles [*Viidanoja et al.*, 2002; *Ho et al.*, 2003; *Fang et al.*, 2008], with little carbonaceous mass in the very coarse fraction of atmospheric particles (>10 μm in diameter). Accordingly, the chemical mass balance was constructed only for PM_{10}, as it is not possible to precisely assign portions of the TSP-derived EC and OC to $PM_{2.5}$ and $PM_{2.5–10}$.

[12] Specific mass contributions of various sources to PM_{10} were calculated using established source reconstruction techniques [*Malm et al.*, 1994; *Brook et al.*, 1997]. The major components considered in our study included minerals (soil), particulate organic matter (POM), elemental carbon (EC), sea salt, trace element oxides, and secondary inorganic particulate species, including sulfates, nitrates, and ammonium.

[13] Typically, crustal elements such as aluminum (Al), silicon (Si), calcium (Ca), iron (Fe), and titanium (Ti) are calculated as oxides, as described by *Malm et al.* [1994] and *Brook et al.* [1997], to estimate the total mineral dust mass, as follows:

$$PM_{mineral} = 2.20\ Al + 2.49\ Si + 1.63\ Ca + 1.58\ Fe + 1.94\ Ti + 1.41\ Potassium\ (K) \quad (1)$$

[14] Silicon content was not measured in this study. This is because the use of hydrofluoric acid (HF) could volatilize silicon as silicon tetrafluoride (SiF_4) during microwave digestion. We thus assumed the Si concentration to be thrice that of the Al concentration, which essentially agrees with Si concentrations measured in soil dust in China in previous studies [*Bi et al.*, 2007]. We also investigated simplifying the estimation of mineral dust contribution by multiplying the Al concentration by a factor of 12.5 [*Hsu et al.*, 2008; *Andreae et al.*, 2008].

$$PM_{mineral} = 12.5 \times Al \quad (2)$$

Interestingly, the results from the two estimation methods were very consistent (Figure 2). For $PM_{2.5–10}$, the mean ratio of the latter method-derived values versus the former method-derived values was 1.06 with a correlation coefficient (R) of 0.99 (n = 102), and for $PM_{2.5}$, the mean ratio was 1.08 with a correlation coefficient (R) of 0.98 (n = 103). The mineral proportions for three $PM_{2.5–10}$ and two $PM_{2.5}$ samples were >100% and therefore were not considered in the regression. The reason for the overestimation of the three $PM_{2.5–10}$ samples was that their PM loadings were low (<10 $\mu g/m^3$), likely leading to larger errors in weighing and, thus, mass contents. However, the overestimation of the two $PM_{2.5}$ samples was likely due to considerably high Al concentrations yet low concentrations of other crustal elements (Ca, Fe, Ti, and K), resulting in the Fe/Al mass ratios being rather low as well (<0.1), as discussed in section 4.6. Note that the results from this study are hence reported based on the simplified, latter estimations.

[15] Sea salt contribution is generally calculated from either sodium ion (Na^+) or Cl^- as follows [*Malm et al.*, 1994; *Ho et al.*, 2003]:

$$PM_{seasalt} = 1.82 \times Cl^- \quad (3)$$

$$PM_{seasalt} = 2.54 \times Na^+ \quad (4)$$

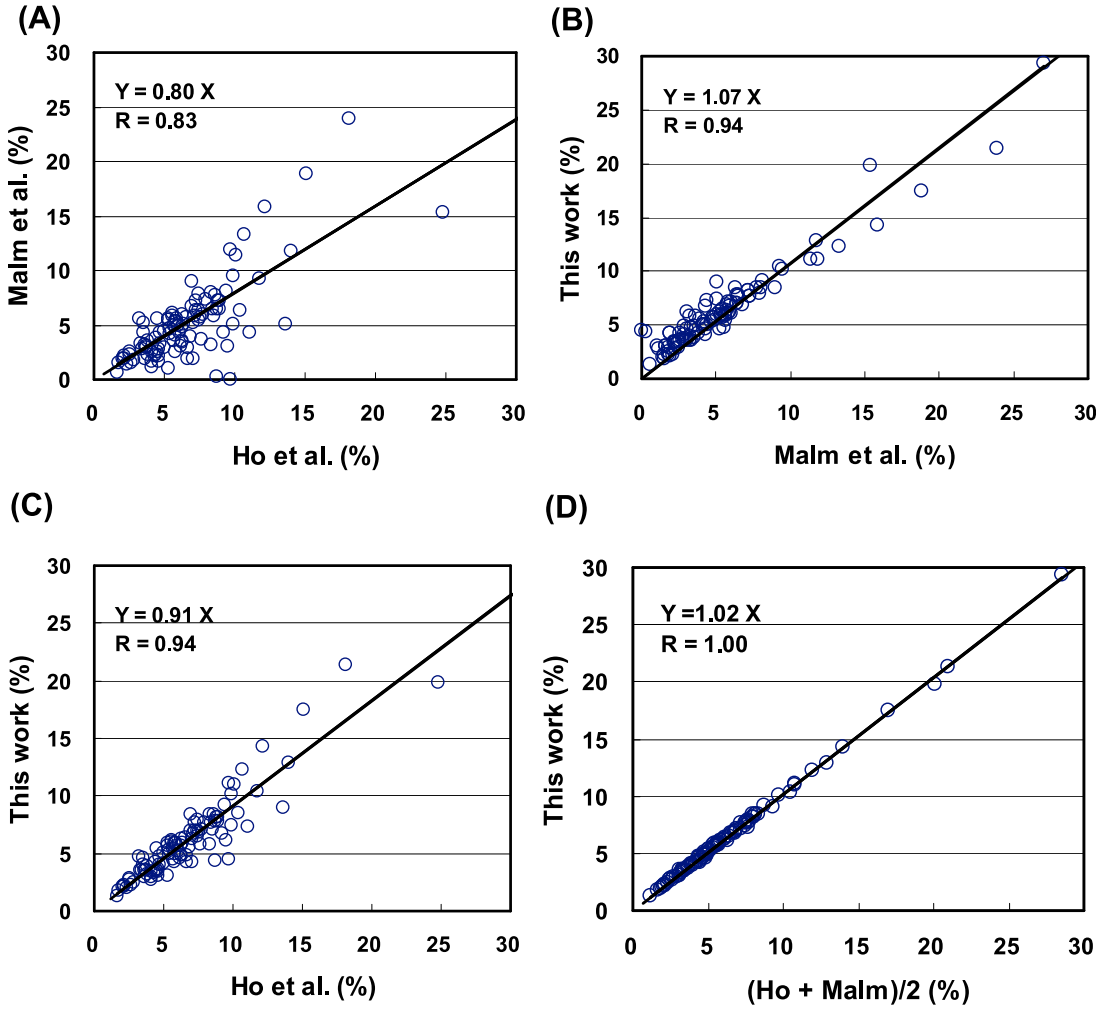

Figure 3. Scatterplots of the estimated sea salt component fractions in PM_{10} Kinmen aerosols obtained by applying three methods (i.e., *Malm et al.*[1994], *Ho et al.* [2003], and our method as described above): (a) Malm et al. versus Ho et al.; (b) ours versus Malm et al.; (c) ours versus Ho et al.; and (d) ours versus half the sum of Malm et al. and Ho et al. (i.e., 1/2 × (Malm et al. + Ho et al.)). Also shown are the linear regression lines forced through zero and equations.

Equation (3) is occasionally corrected with a factor of 0.89 when considering chloride depletion due to acid substitution [*Seinfeld and Pandis*, 1998]. However, we defined $PM_{seasalt}$ as the total concentration of Cl^-, Na^+, and magnesium ion (Mg^{2+}), which is similar to that used by *Sciare et al.* [2003] (seasalt = $Na^+ + Cl^- + ss\text{-}SO_4^{2-} + ss\text{-}Ca^{2+} + Mg^{2+} + ss\text{-}K^+$). As a consequence, results derived from equations (3) and (4) are moderately consistent with each other (Figure 3a); the former being 80% of the latter with a correlation of R = 0.83. On the other hand, our results may have a certain over- or underestimation when compared to the results derived from the two methods cited here (Figures 3b and 3c). However, results derived from using our definition of sea salt are almost equal to the average values derived from the two methods, with a mean ratio of 1.02 and an excellent correlation coefficient of R = 1.00 (Figure 3d). This supports the validity of our method, even though we realize that a portion of water-soluble chloride, sodium, and magnesium might originate from anthropogenic sources (in the case of chloride) and/or mineral soils (in the case of sodium and magnesium).

[16] In previous studies [e.g., *Viidanoja et al.*, 2002, and references therein], particulate organic matter (POM) was calculated as follows:

$$POM = 1.6 \times OC \tag{5}$$

The conversion factor from OC to POM used here is 1.6 [*Viidanoja et al.*, 2002], whereas in other investigations factors were used with a wide range from 1.4 to 2.2 [*Cass et al.*, 2000; *Turpin and Lim*, 2001; *Edgerton et al.*, 2005; *Andreae et al.*, 2008]. The determinants for choosing a suitable factor are relatively complex [*Turpin and Lim*, 2001]. Considering the influence of urban and industrial PM sources on our study location, we adopted a value of 1.6.

Table 1. Summary of Enrichment Factor Values for Trace Elements in PM_{10} Kinmen Aerosols

	Range	Mean ± S.D.[a]
Co	0.1–2.4	0.9 ± 0.4
Y	0.04–2.6	0.8 ± 0.5
Sr	0.1–12.9	1.4 ± 1.7
Ba	0.3–33.2	3.4 ± 5.2
Mn	0.3–6.5	2.1 ± 1.3
Rb	0.3–11.8	3.5 ± 2.1
Ni	0.3–2.7	1.3 ± 0.5
Cr	1.2–13.8	3.9 ± 2.4
V	0.2–8.0	1.7 ± 1.4
Cu	6.9–133	23 ± 17
Zn	17–753	183 ± 146
Mo	3.8–193	39 ± 32
Cd	76–3066	756 ± 551
Sn	41–1276	269 ± 206
Sb	156–3350	1163 ± 772
Tl	11–371	72 ± 52
Pb	51–1599	420 ± 300
As	23–677	185 ± 146
Se	1020–28303	5305 ± 3818
Ge	3.8–92	24 ± 17
Cs	1.2–66.8	13.1 ± 9.2
Ga	2.2–51.6	16.6 ± 10.1

[a]One standard deviation.

[17] *Landis et al.* [2001] determined the mass contribution of trace element oxides as follows:

$$\begin{aligned}\mathrm{TEO} = {} & 1.47\ \mathrm{Vanadium\ (V)} + 1.29\ \mathrm{Manganese\ (Mn)} \\ & + 1.27\ \mathrm{Nickel\ (Ni)} + 1.25\ \mathrm{Copper\ (Cu)} \\ & + 1.24\ \mathrm{Zinc\ (Zn)} + 1.32\ \mathrm{Arsenic\ (As)} \\ & + 1.08\ \mathrm{Lead\ (Pb)} + 1.20\ \mathrm{Selenium\ (Se)} \\ & + 1.37\ \mathrm{Strontium\ (Sr)} + 3.07\ \mathrm{Phosphorous\ (P)} \\ & + 1.31\ \mathrm{Chromium\ (Cr)} + 1.41\ \mathrm{K}\end{aligned}$$

Following *Landis et al.* [2001], we also estimated the contribution of heavy metals as metal oxides by employing the following equation, considering additional trace metals which have been analyzed in our studies and thus their enrichment factors (EFs) have been calculated:

$$\begin{aligned}\mathrm{TEO} = {} & 1.3 \times [0.5\ \mathrm{Sr} + 0.5\ \mathrm{Barium\ (Ba)} + 0.5\ \mathrm{Mn} \\ & + 0.5\ \mathrm{Rubidium\ (Rb)} + 0.5\ \mathrm{Ni} + 0.5\ \mathrm{Cr} + 0.5\ \mathrm{V} \\ & + \mathrm{Cu} + \mathrm{Zn} + \mathrm{Molybdenum\ (Mo)} + \mathrm{Cadmium\ (Cd)} \\ & + \mathrm{Tin\ (Sn)} + \mathrm{Antimony\ (Sb)} + \mathrm{Thallium\ (Tl)} \\ & + \mathrm{Pb} + \mathrm{As} + \mathrm{Se} + \mathrm{Germanium\ (Ge)} + \mathrm{Cesium\ (Cs)} \\ & + \mathrm{Gallium\ (Ga)}]\end{aligned}$$

We calculated the EFs of the analyzed metals in PM_{10} as follows:

$$\mathrm{EF_{crust}} = (\mathrm{C_X}/\mathrm{C_{Al}})_{\mathrm{aerosol}}/(\mathrm{C_X}/\mathrm{C_{Al}})_{\mathrm{crust}}$$

where $(C_X/C_{Al})_{aerosol}$ is the concentration ratio of a given element X to Al in aerosols, and $(C_X/C_{Al})_{crust}$ is the concentration ratio of a given element X to Al in the average crustal abundance [*Taylor*, 1964]. The degree to which the element X in an aerosol sample is enriched or depleted relative to a specific source (e.g., average crust) can be assessed using EF values. Depending on the EFs (Table 1), all analyzed trace elements were considered in different weights. Elements having enrichment factors of ≤1.0, such as cobalt (Co) and yttrium (Y), were not taken into account in the calculation, as they were identified to be of exclusive crustal origin. Elements having EFs between 1 and 5 were multiplied by a factor of 0.5, as they were identified as originating from two sources, (i.e., anthropogenic and crustal sources). Elements having EFs of ≥5.0 were multiplied by unity as they were identified to be dominated by anthropogenic origins. Furthermore, the multiplicative factor was simply set to 1.3, such that the metal abundance would be converted to oxide abundance when considering those used by *Landis et al.* [2001], when no adequate literature information on metal speciation was available for evaluation. Therefore, note that here we report only the results of the heavy metal oxide components using our equation.

[20] The secondary inorganic species, sulfate, nitrate, and ammonium, were considered individually. Also, we must note that a fraction of the sulfate concentration was of sea salt origin, and a portion of the nitrate might be the product of heterogeneous reactions between nitric acid and sea salt aerosol. Nevertheless, both sulfate and nitrate were considered as secondary particulate species.

3.5. Air Mass Backward Trajectory Analysis

[21] We calculated 48-h air mass back trajectories using the NOAA Hybrid Single Particle Lagrangian Integrated Trajectory (HYSPLIT) model with a 1° × 1° latitude-longitude grid and the final meteorological database. The 6-hourly final archive data were generated from the National Center's for Environmental Prediction (NCEP) Global Data Assimilation System (GDAS) wind field reanalysis. GDAS used a spectral medium-range forecast (MRF) model. More details about the HYSPLIT model can be found at http://www.arl.noaa.gov/ready/open/hysplit4.html (NOAA Air Resources Laboratory).

4. Results and Discussion

4.1. A Year-Long Air Mass Trajectory Analysis

[22] Air mass trajectories at two elevations of 50 and 500 m between December 2007 and November 2008 were analyzed using the HYSPLIT model. Results for 50 m trajectories are depicted on a seasonal basis in Figure 4. As the 500 m trajectories were essentially consistent with the 50 m trajectories, they are not shown here. During the northeasterly monsoon season (i.e., generally from late September to mid-May), air masses are primarily advected from north-to-northeast, originating on the Asian continent and passing along East China's coastal line. This is particularly true in winter. Nevertheless, air masses may occasionally (mainly in spring and fall) be transported over oceanic areas as well. In contrast, southeast winds with a maritime origin prevail in summer. Consequently, the study area, Kinmen Island, is expected to be substantially affected by the outflow of air pollution from the Asian continent associated with the northeasterly monsoon.

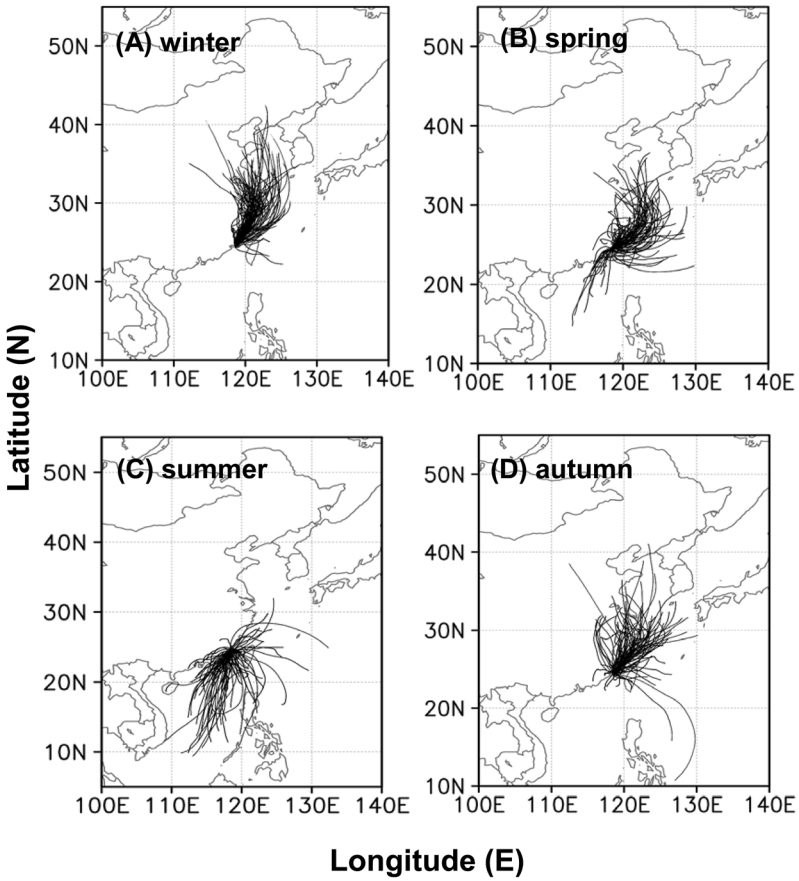

Figure 4. The 48-h air mass backward trajectories at 50 m above ground level for the period between December 2007 and November 2008. They were analyzed using the NOAA HYSPLIT model. Presented here are the results from: (a) winter, (b) spring, (c) summer, and (d) autumn.

4.2. Air Pollution During the Winter Monsoon

[23] Based on the data set obtained from the EPA of Taiwan, monthly and seasonal variations in the monitored species, such as PM_{10}, SO_2, CO, and NO_x, were constructed and shown in Figures 5 and 6, respectively. Several features in terms of seasonality were identified: (1) All selected species peaked in the winter and spring months, when the northeasterly monsoon prevailed, and decreased in the summer months, when southeasterly winds prevailed; meanwhile, concentrations in autumn were high only on occasion. (2) Concentrations in the recent three years (2006 to 2008) appear to be relatively higher than in the two preceding years (2004 and 2005). (3) Monthly PM_{10} concentrations in the recent three years frequently exceeded 100 $\mu g/m^3$ during the northeasterly monsoon months, revealing an apparent increase in PM pollution, which needs to be verified in the future. Surprisingly, the monthly average PM_{10} concentration in March of 2008 at Kinmen was rather high at 150 $\mu g/m^3$, exceeding the Taiwan National Ambient Air Quality Standard (125 $\mu g/m^3$) for 24-h average PM_{10} and being 2.3 times higher than the USA National Ambient Air Quality Standard for 24-h average $PM_{2.5}$ levels (i.e., 65 $\mu g/m^3$). Moreover, the daily PM_{10} concentrations in the aerosol-sampling period between December 2007 and February 2008 exceeded Taiwan's (or USA's) 24-h air-quality standard on 32 (or 76) days. Such levels and seasonal patterns were very similar to those measured in Hangzhou City, Zhejiang Province, eastern China [*Cao et al.*, 2009], located ~600 km north of our sampling site.

[24] For comparison, the monthly patterns of these species at the industrial site, Linyuan, which is located outside a petrochemical park in Southern Taiwan (Figure 1b), are also shown in Figure 5. Surprisingly, levels and distributions of monthly concentrations of PM_{10}, SO_2, and CO in Kinmen are quite similar to those at Linyuan. PM_{10} concentrations in Kinmen were gradually approaching or even exceeding those at Linyuan. Another feature of the PM_{10} concentrations is that the background, summertime concentrations (around 30 $\mu g/m^3$) in Kinmen were obviously lower than those (around 40 $\mu g/m^3$) at Linyuan. The most distinct difference between the two sites exists in NO_x, which is much higher at the urban/industrial site of Linyuan, than at the rural site of Kinmen. Such high NO_x concentrations at the industrial site are due to proximity to fresh emissions from combustion sources which may include both mobile and stationary sources, which were prevalent at Linyuan. Accordingly, this comparison highlights the magnitude of the air pollution problems especially the PM levels in Kinmen. Based on the results of the air mass trajectory analyses, the high PM levels over Kinmen Island were likely due to areal- to

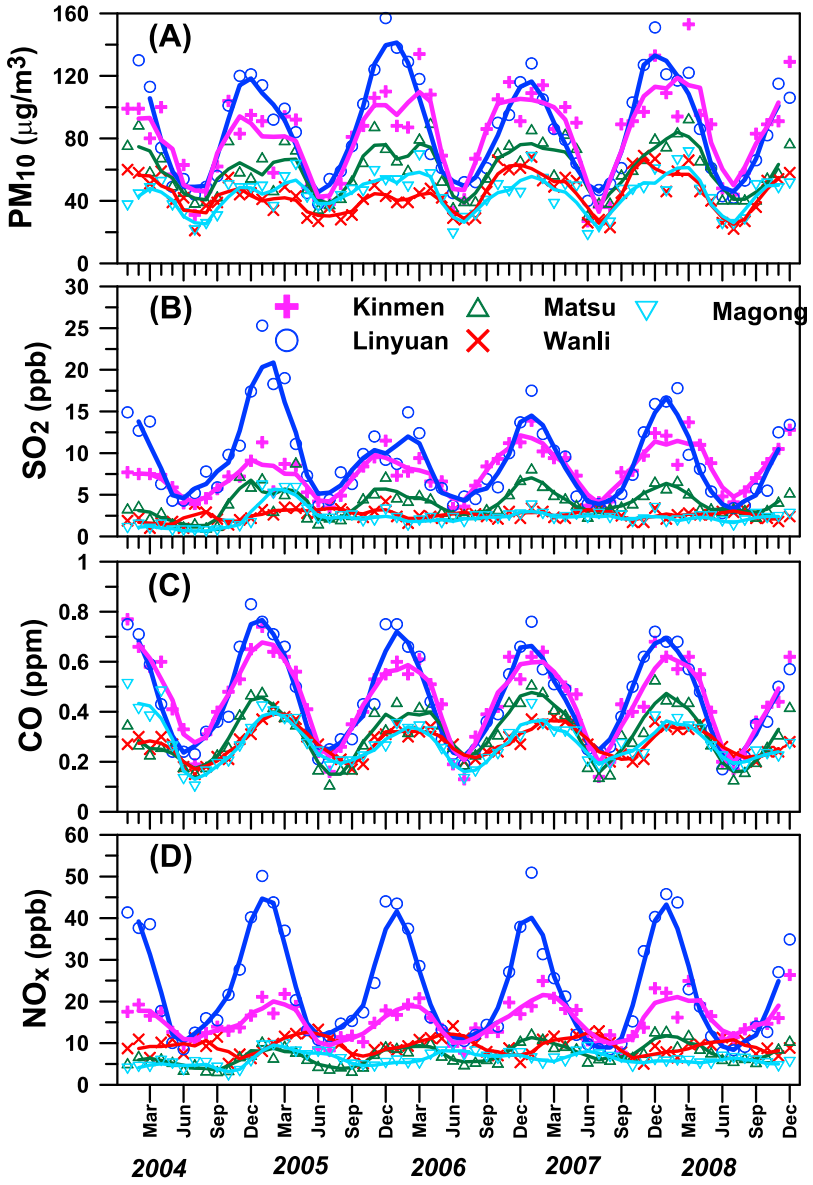

Figure 5. Monthly variations of (a) PM_{10}, (b) SO_2, (c) CO, and (d) NO_x from January 2004 to December 2008 measured on Kinmen Island (pink cross) by the Taiwan EPA. For comparison, the respective patterns from four other sites (Linyuan, Matsu, Wanli, and Magong) are also displayed for the same time period.

regional-scale transport of polluted air masses from the northeast.

[25] For further evaluation of the influence of regional LRT on the high PM levels in Kinmen, we compared the monthly variations in PM with those observed at three other sites: Wanli, Magong, and Matsu. These three sites were influenced by LRT of continental pollution from Asia during the northeasterly monsoon [*Junker et al.*, 2009]. As shown in Figure 5, the similar seasonal trends in air quality parameters at all these sites highlight the regional nature of the air pollution problem. The Kinmen site, though not near significant local sources, was particularly impacted by high levels of PM_{10}, SO_2 and CO, comparable to those observed at the highly industrial Linyuan site. These findings suggest that Kinmen was impacted mainly by trans-boundary transport of air pollutants, along with LRT of pollutants from regional sources, which is also demonstrated by the air mass trajectories (Figure 4). Therefore, we further quantitatively evaluated the influence of regional LRT from northern China and the YRD.

[26] Because Kinmen is approximately located in between the two background air-quality stations, Wanli and Magong, data from these two stations were used for reference. The differences (21.1 $\mu g/m^3$ for Wanli and 21.7 $\mu g/m^3$ for Magong) in PM_{10} concentrations between the northeasterly winter (49.7 ± 10.3 $\mu g/m^3$ for Wanli and 49.5 ± 8.8 $\mu g/m^3$ for Magong) and summer (28.6 ± 5.7 $\mu g/m^3$ for Wanli and 27.8 ± 6.9 $\mu g/m^3$ for Magong) monsoons during the study period (2004–2008) were nearly identical, suggesting that this value (21 $\mu g/m^3$) could be regarded as the regional

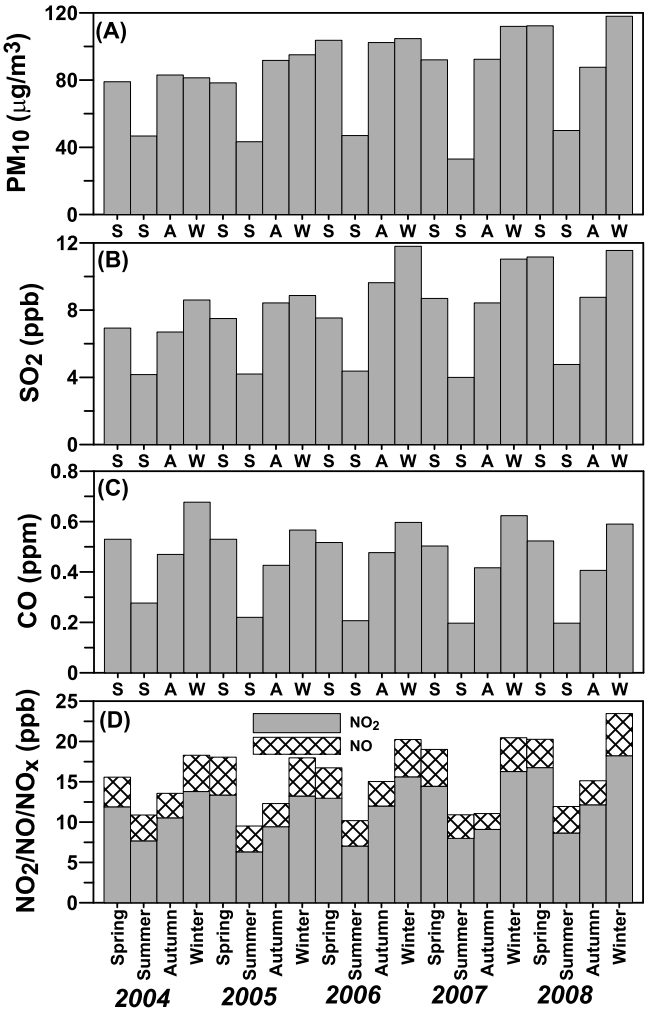

Figure 6. Seasonal variations of (a) PM_{10}, (b) SO_2, (c) CO, and (d) NO_x (i.e., sum of NO and NO_2) between January 2004 and December 2008 measured on Kinmen Island by the Taiwan EPA. Spring is denoted as S, summer S, autumn A, and winter W.

influence on the study area. Hence, we estimated the contribution of regional LRT to the PM levels (95 $\mu g/m^3$) during the northeasterly monsoon on Kinmen Island to be 22% on average, indicating that PM pollution in Kinmen was not dominated by regional-scale LRT. In regards to Asian dust, which is mainly derived from northern China's deserts and the Gobi Desert, according to our recent studies [*Hsu et al.*, 2008], the contribution of Asian dust to ambient PM levels in the region south of 25°N is only ~3.5 $\mu g/m^3$ on average during the northeastern monsoon, indicating that Asian dust does not constitute an important source of aerosols in Kinmen either.

4.3. Diurnal Patterns in Wintertime Pollution

[27] As depicted in Figure 7, we further analyzed the hourly variations in a day for PM_{10}, $PM_{2.5}$, SO_2 and wind speed during the winter when the aerosol filter samples were collected (i.e., from December 2007 to February 2008). The outlier data points shown in each plot highlight the extreme data and thus the air-quality deterioration. Again, we found several crucial features as follows: (1) Extreme PM_{10} concentrations, arbitrarily defined as double the 24-h PM standard in Taiwan (i.e., 2 × 125 $\mu g/m^3$), occurred predominantly in the morning hours, around 7:00 A.M. to 10:00 A.M. local time (local time is used throughout this paper). In a few cases, this spike was observed in the second half of the day (i.e., 12:00 P.M.–12:00 A.M.). (2) Interestingly, extreme $PM_{2.5}$ concentrations seemed to occur later in the day (i.e., 9:00 A.M. to 12:00 P.M.). (3) In contrast, extreme SO_2 concentrations occurred slightly earlier than the former two species and spanned a longer period of the day (i.e., 6:00 A.M. to 12:00 P.M.). (4) Wind speed usually decreased in early morning, around 4:00 A.M. to 7:00 A.M. In particular, note that even though the median (50%) wind speed was minimal at 5:00 A.M., the 75% (low end of each box) value was also minimal at 6:00 A.M. In other words, the circulation may have become nearly stagnant with abnormally low wind speeds of less than 2 m/s during the morning hours. Briefly, the peaks in the PM and SO_2 levels during the morning hours (7:00–10:00 A.M.) were often associated with low wind velocities and likely low mixing layer heights, which resulted in poor ventilation [*Krishnan and Kunhikrishnan*, 2004]. However, the relative roles in the contributions of primary versus secondary aerosols are not fully understood from the present data set, as discussed by *Brock et al.* [2008].

4.4. Case Studies of High PM Episodes in Winter

[28] In order to further explore the high wintertime PM episodes in Kinmen, two cases were selected for analysis in detail: 6–9 December 2007 and 5–8 January 2008. Figures 8 and 9 illustrate the hourly variations of PM_{10} and $PM_{2.5}$, as well as SO_2, CO, NO_2/NO_x, temperature, relative humidity, and wind speed and direction during these periods.

[29] During the period of 6–9 December 2007 (Figure 8), the PM_{10} maximal hourly concentration reached nearly 600 $\mu g/m^3$ at 6:00 A.M. on 7 December, while the corresponding maxima in SO_2 and NO_x/NO_2 appeared earlier (at 5:00 A.M.), with the CO maximum occurring later (at 8:00 A.M.). Note that the $PM_{2.5}$ concentration at the peak time was <200 $\mu g/m^3$, i.e., coarse aerosols ($PM_{2.5-10}$) dominated the PM burden. At that time, the prevailing winds were from the NE and had low speeds of less than 2 m/s. In the case 5–8 January 2008 (Figure 9), three hourly PM_{10} spikes of >400 $\mu g/m^3$ took place at 8:00 A.M. on 5 January, 10:00 A.M. on 7 January, and 9:00 A.M. on 8 January. In these cases $PM_{2.5}$ mass accounted for ~35%, ~40%, and ~45% (i.e., all <50%) of the PM_{10} peak levels, respectively. In contrast to the former case, peaks in SO_2, CO, and NO_x concentrations were concurrent with those in PM_{10}, except on 5 January, when no corresponding SO_2 maximum was observed. Also, winds were weak in this case, and blew mainly from the northern to northeastern direction, similar to the former case. In summary, we may conclude that the high PM levels in Kinmen were primarily due to the transport of polluted air masses from north to northeast of the island and ineffective dispersion due to the decreased wind speeds and lower mixing layer height, resulting in rapid accumulation of air pollutants [*Krishnan and Kunhikrishnan*, 2004].

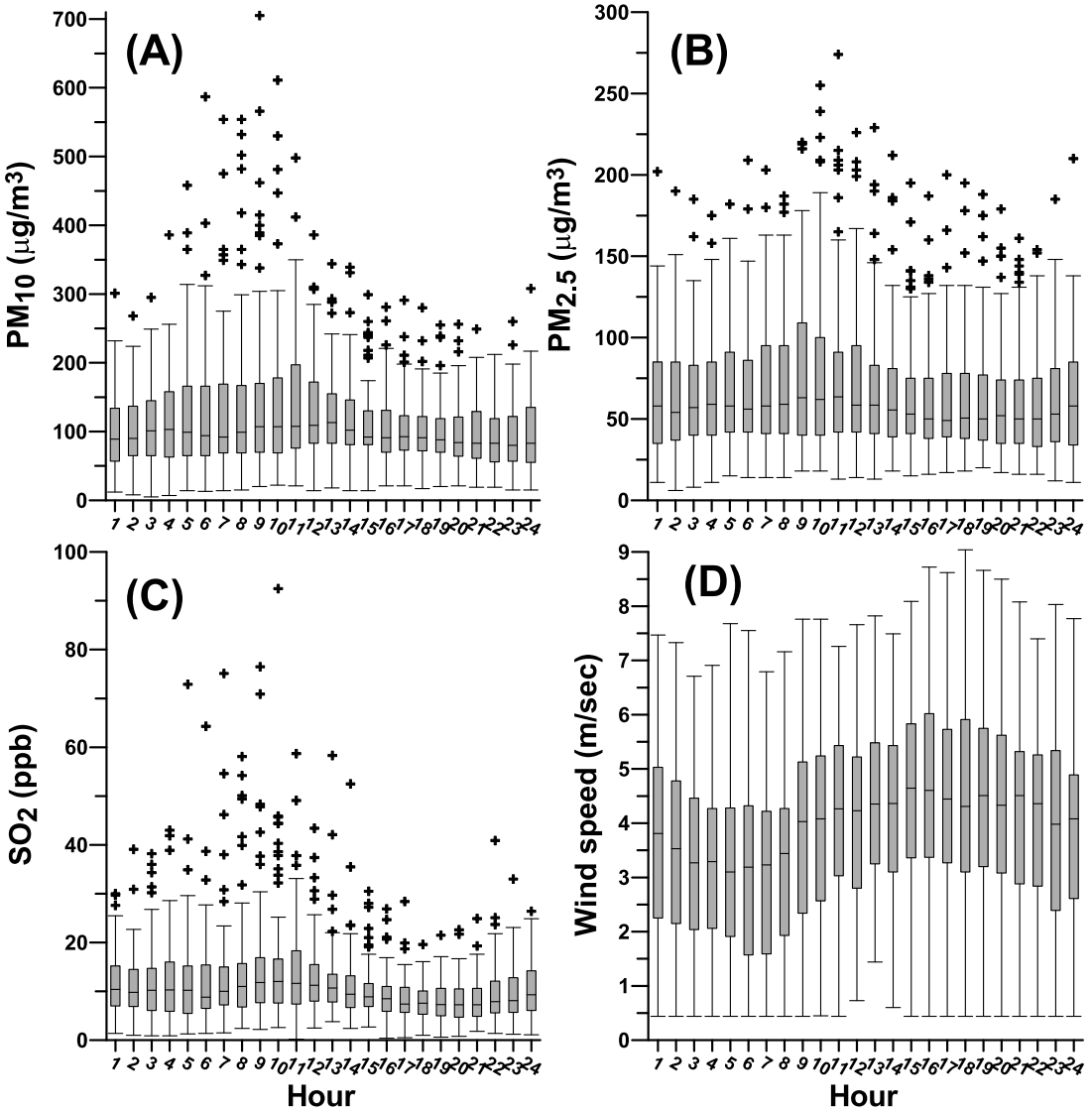

Figure 7. Hourly variability of (a) PM_{10}, (b) $PM_{2.5}$, (c) SO_2, and (d) wind speed during the wintertime between December 2007 and February 2008 in Kinmen. In the plots, the ends of the box, the ends of the whiskers, and the line across each box represent the 25th and 75th percentiles, the 5th and 95th percentiles, and the median, respectively. Crosses indicate data outliers representing extreme data.

4.5. Main Chemical PM Components

[30] During the sampling period between 22 November 2007 and 6 March 2008, our gravimetrically derived daily $PM_{2.5}$ and $PM_{2.5–10}$ concentrations averaged 39 and 26 $\mu g/m^3$, respectively, with a mean C/F (coarse to fine mode aerosol) mass ratio of 0.67.

[31] Based on the chemical analysis of these aerosol samples, the major components of PM_{10} aerosols included sulfate (23.7 ± 7.2%), mineral particles (18.6 ± 5.9%), and particulate organic matter (POM, 18.5 ± 6.8%). The minor components were ammonium (7.5 ± 2.2%), nitrate (5.1 ± 2.1%), sea salt (4.9 ± 1.7%), EC (2.7 ± 1.3%), and heavy metal oxides (0.9 ± 0.2%). Unidentified components accounted for a significant portion (17.9%) of the PM mass (Figure 10). Note that we have assumed that OC and EC contents measured in TSP filter samples could represent their exclusive association with PM_{10} aerosol particles [*Chou et al.*, 2005; *Fang et al.*, 2008]. Interestingly, the three main PM components, i.e., sulfate, mineral species, and POM, made up the majority of the bulk aerosol, while sea salt comprised only a minor fraction, which was similar to observations made in the USA [*Malm et al.*, 2004], even though our study location was on an island (i.e., coastal area). Also, the patterns observed during our study were similar to those observed in Hangzhou City, Zhejiang Province, Eastern China [*Cao et al.*, 2009]. Noticeably, nitrate accounted for a modest fraction (5.1%) of all chemical species, which was substantially lower (12%) than in the urbanized city, Hong Kong [*Yuan et al.*, 2006]. Trace element oxides represented only 0.9% of Kinmen PM_{10}, whereas *Cass et al.* [2000] found that their proportion could reach 14% in ultrafine particles.

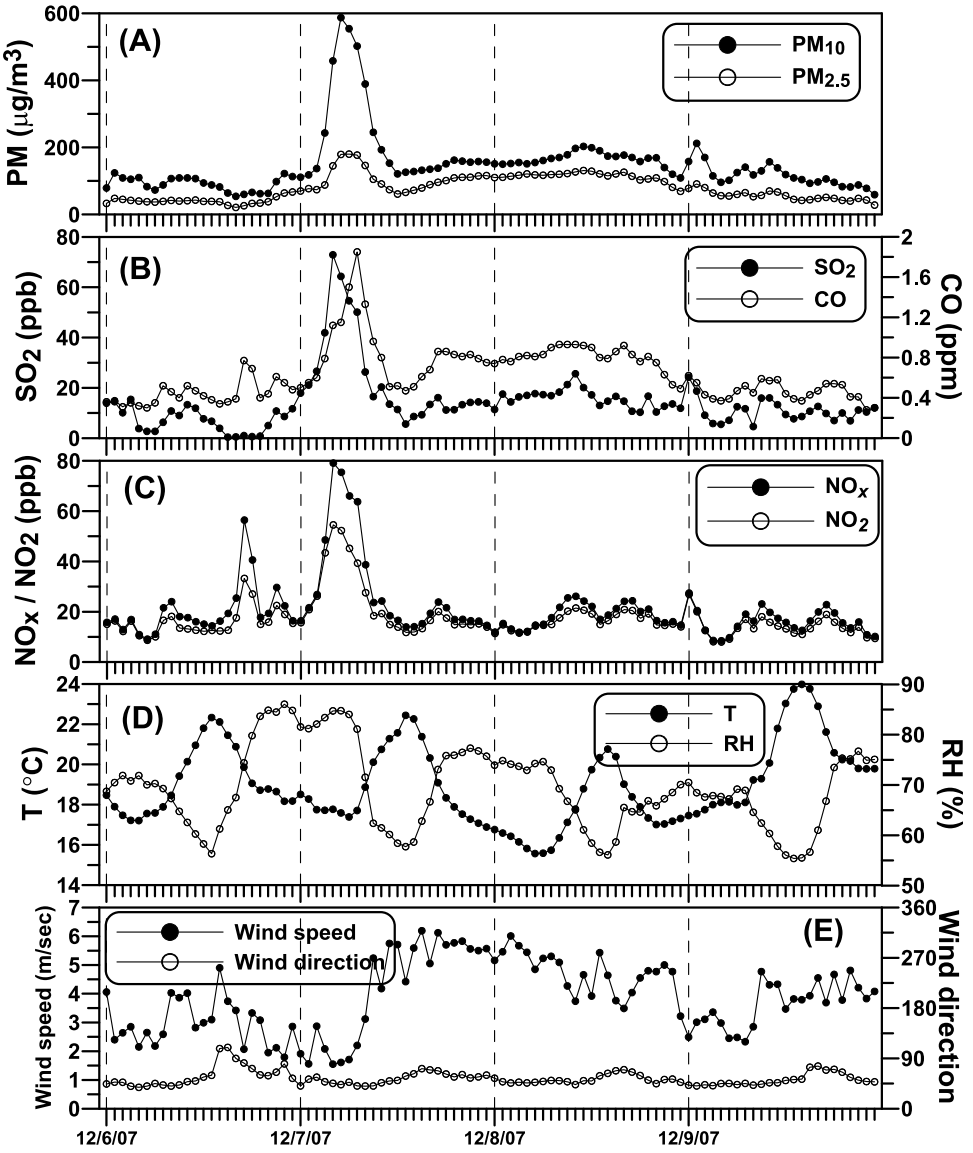

Figure 8. Hourly variations of (a) PM_{10} and $PM_{2.5}$, (b) SO_2 and CO, (c) NO_2 and NO_x, (d) temperature and relative humidity (RH), and (e) wind direction and speed for the selected high PM episode in the four-day period between 6 and 9 December 2007. Vertical dashed lines indicate the first hour (local time) of each day.

Nevertheless, if inhaled, certain transition metals may act as biochemical catalysts and cause molecular damage, even when present at lower ambient levels [*Lingard et al.*, 2005].

[32] As shown above, we noticed that the variability in the proportion for each component is relatively small (all <50%) during the sampling period despite the variability in the atmospheric concentrations of PM and chemical species being rather large (up to one order of magnitude or more). This implies a somewhat constant mix of regional sources during the northeasterly monsoon (i.e., during winter). As mentioned above, there were only a few industrial activities on the investigated island, suggesting that distant sources, rather than local ones, contributed to the measured anthropogenic substances.

[33] Furthermore, the mean concentrations of all analyzed chemicals in PM_{10} (i.e., total of $PM_{2.5-10}$ and $PM_{2.5}$) are reported here, as depicted in Figure 11. Overall, the concentrations of most species were higher than those measured in rural areas, and are even comparable with those observed at industrial sites around the world, particularly in developed countries [*Chester et al.*, 2000; *Malm et al.*, 2004; *Hueglin et al.*, 2005; *Koulouri et al.*, 2008]. For instance, the mean concentration for nss-sulfate was 16 $\mu g/m^3$ and ammonium averaged at 5.0 $\mu g/m^3$, substantially higher than those ($\leq$6 $\mu g/m^3$ for ammonium sulfate) observed in the USA [*Malm et al.*, 2004]. Note also that the mean concentrations for heavy metals, such as Zn, Pb, Cu, Cr, Sn, As, Cd, Sb, Se, Mo, and Ga were rather elevated; among them, As, Se, and Ga are mostly attributed to coal combustion [*Xu et al.*, 2004]. Also noticeable was the high average concentration of fluoride (144 ng/m^3), which was significantly higher than typical levels of fluoride in rural and urban

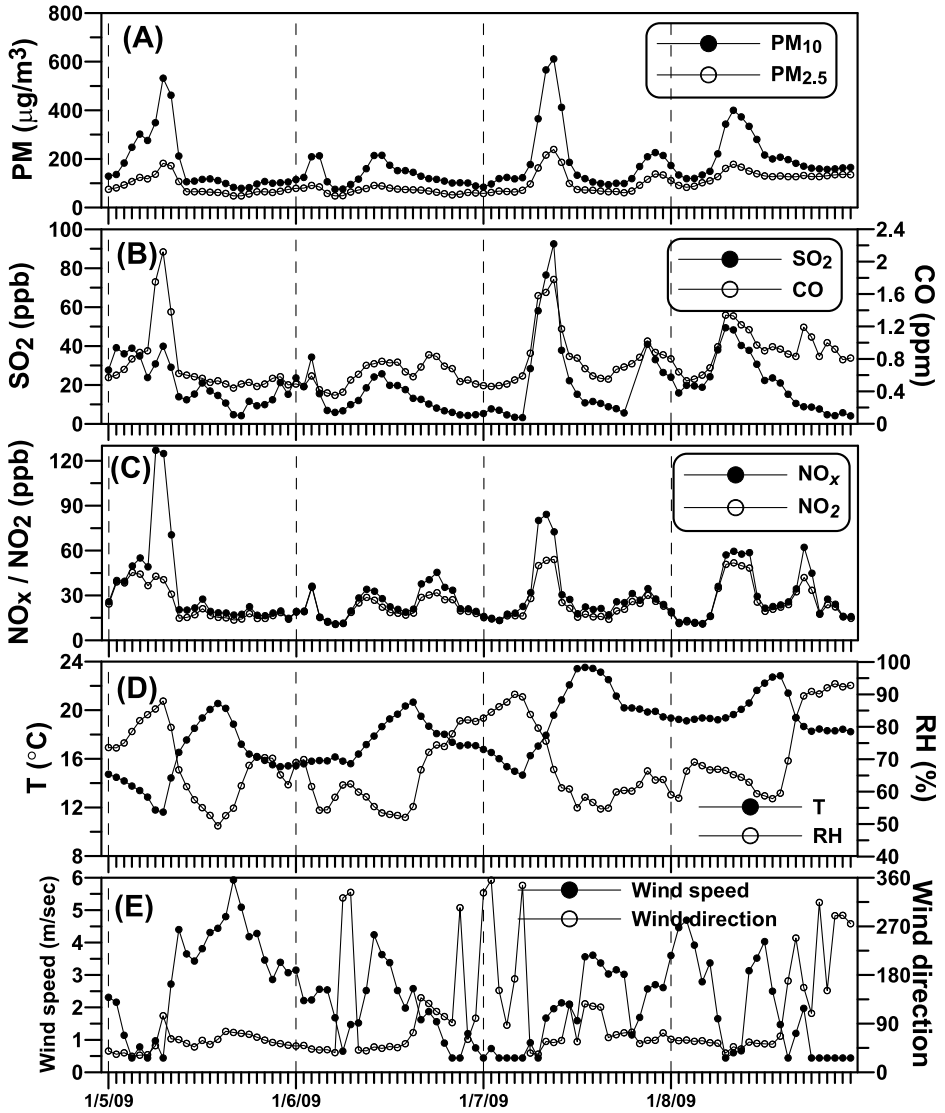

Figure 9. Hourly variations of (a) PM_{10} and $PM_{2.5}$, (b) SO_2 and CO, (c) NO_2 and NO_x, (d) temperature and relative humidity (RH), and (e) wind direction and speed for the selected high PM episode in the four-day period between 5 and 8 January 2008. Vertical dashed lines indicate the first hour (local time) of each day.

areas, which at times are even below analytical detection limits. The high fluoride concentrations may also be related to coal combustion in upwind areas [*Ando et al.*, 2001; *Xu et al.*, 2004].

4.6. Sources of High PM in Kinmen

[34] As depicted in Figure 12a, Fe and Al showed excellent correlations in both $PM_{2.5–10}$ and $PM_{2.5}$ aerosol particles, and the mean Fe/Al mass ratios were 0.43 in $PM_{2.5–10}$ and 0.21 in $PM_{2.5}$. When compared to the average crust composition (0.68 [*Taylor*, 1964]), Chinese loess (0.57 [*Zhang et al.*, 2003]), and Chinese desert dust (0.44–0.83 [*Zhang et al.*, 1997]), Fe/Al mass ratios in Kinmen aerosols were quite low. In order to examine if the dust aerosols fraction was composed of local soil dust, we analyzed soil samples collected from five sites around 2 km from the aerosol sampling station. Fe/Al mass ratios in local soil dusts ranged from 0.47 to 0.56, confirming little influence of local soils.

[35] Interestingly, Fe/Al ratios in aerosols, particularly $PM_{2.5}$, were very close to those (0.10–0.15) measured in fugitive dust aerosols collected within the ceramic manufacturing factories in Guangzhou, south China (C.Y. Chan's unpublished data). More importantly, the low Fe/Al ratio (0.21) in Kinmen $PM_{2.5}$ aerosols was very similar to that (average 0.20) measured in four sets of size-resolved aerosols collected from Cizao Town, Jingjiang City in April 2009 (Figure 12b), which is the most important area producing architectural pottery materials (e.g., tiles), named as "ceramic town of China." Additionally, the size distribution of both Al and Fe displayed a bimodal pattern (not shown), peaking at 5.6–10 and 1.0–1.8 μm, which was different from that (mono-modal pattern) observed in Taipei [*Hsu et al.*, 2009b]. The average mass median

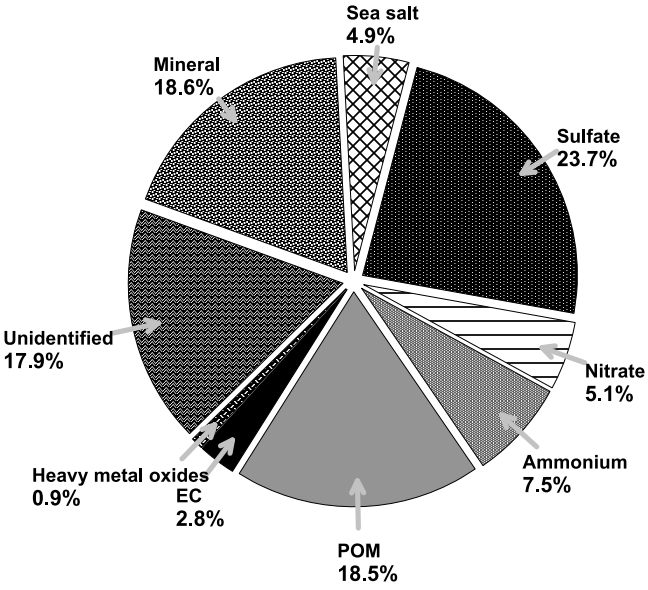

Figure 10. A pie-chart showing the average components of PM_{10} aerosols based on chemical analysis results of all filter samples collected in this study. Numbers indicate the proportions (%) for each component.

diameter (MMD) of Al was only 1.8 μm, which is also significantly smaller than that (3.6 μm) observed in Taipei [*Hsu et al.*, 2009b], thus facilitating LRT. The reason why the Fe/Al ratios in ceramic dust aerosols are so low is that clays, being the chief material of ceramic products, are composed mostly of kaolinite, $Al_2O_3{\cdot}2SiO_2{\cdot}2H_2O$, which contains low Fe. Therefore, fugitive dust emitted from the nearby ceramic manufacturing plants is likely one of the main sources of ambient PM in Kinmen.

[36] According to *Querol et al.* [2007], aerosols in the glazed ceramic production areas in Spain are characterized by high levels of Zn, As, Se, zirconium (Zr), Cs, Tl, lithium (Li), Co, and Pb. Interestingly, aside from high levels of Zn, Pb, As, Se, and Tl in our samples, Cs, which is usually recognized as a typical crustal element, had a high enrichment factor of ~10 relative to average crust composition, indicating a non-dust source and, thus, likely ceramic-related sources. Additionally, other chemical evidence that supports this indication includes the observations of high nss-sulfate, along with high volatile metals, such as As and Se, as well as high fluoride, which mainly originate from coal combustion [*Xu et al.*, 2004; *Cao et al.*, 2009]. This is reasonable because large quantities of coke may be used as energy sources in pottery/porcelain manufacturing.

[37] Fujian Province is well known as one of the five famous traditional pottery/china-producing areas in China. Fujian, Jinjiang City, which is located 40–50 km northeast of Kinmen Island (Figure 1a), hosts the most important area of architectural ceramic/porcelain products, of which wall and glazed tiles dominate the national production in China (65% for wall tiles and >90% for glazed tiles in China) (http://unn.people.com.cn/GB/22220/39486/6624407.html). Consequently, Jinjiang City is likely the key source area contributing to the high PM levels on Kinmen Island in the northeasterly monsoon, although this requires further investigation. In addition to architectural ceramic materials, Jinjiang City is a very important area for producing sports shoes and jackets, with a contribution to the worldwide production of 20% and 21%, respectively (http://unn.people.com.cn/GB/22220/39486/6624407.html).

[38] Note that high POM contents averaging 18.5% of the bulk PM_{10}, and moderate OC/EC mass ratios averaging at 4.4 (Figure 13a), were measured in the Kinmen aerosols. This mean ratio was close to the average value (3.8), which was observed in 14 cities across China in winter [*Cao et al.*, 2007] during the same season (winter) as our sampling time. These OC/EC ratios approximately fall within the range between aerosols influenced by biomass burning (≥5) [*Ryu et al.*, 2004] and traffic exhaust (≤2.0) [*Watson et al.*, 1994]. An OC/EC ratio of ≥2.0–2.2 has been adopted to indicate the presence of secondary organic aerosols in earlier studies [*Turpin et al.*, 1990; *Chow et al.*, 1996], while ratios below this threshold are considered to signify aerosol which was primarily derived from fossil fuel combustion. Consequently, the relatively high OC/EC ratio (4.4) observed here suggests that traffic emissions may not have been the predominant

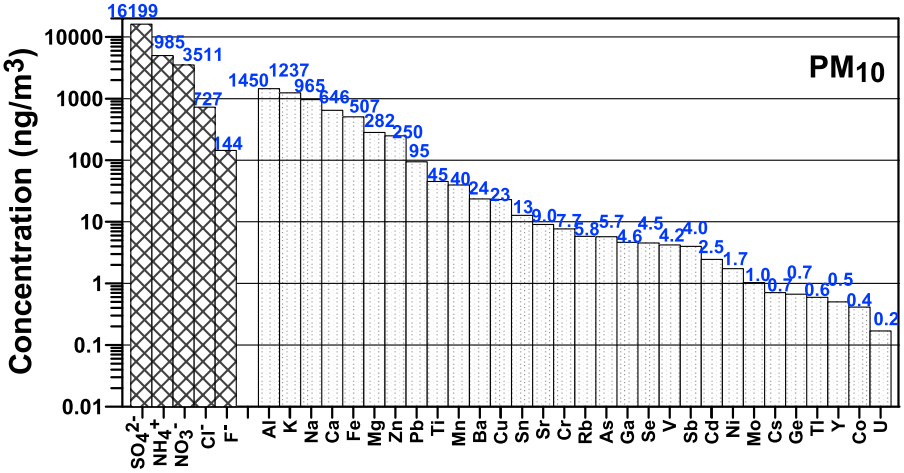

Figure 11. Mean wintertime concentrations (in ng/m^3) for each analyzed chemical species (ions and metal elements) in the PM_{10} filter samples.

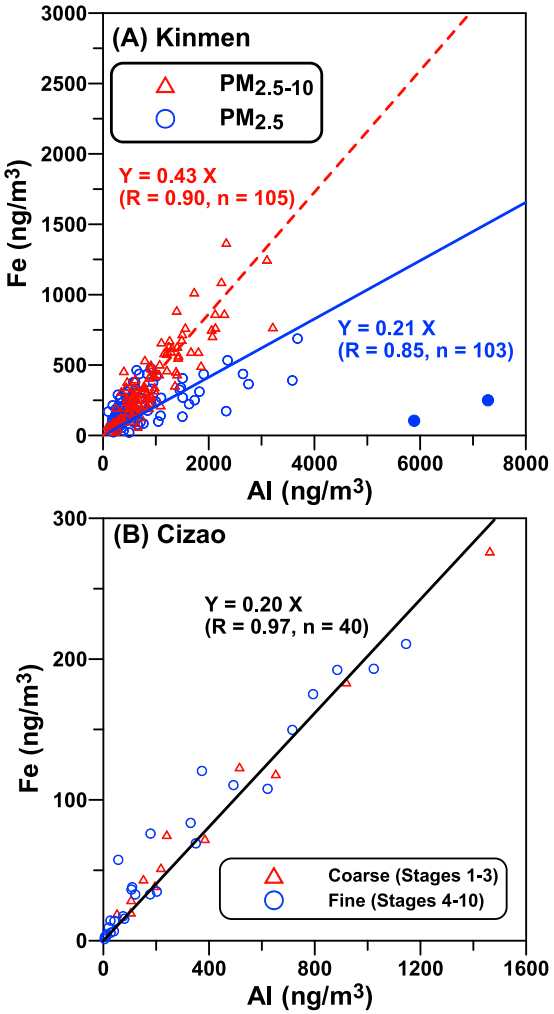

Figure 12. Correlations between Fe and Al in (a) $PM_{2.5–10}$ and $PM_{2.5}$ aerosols in Kinmen and (b) the 10-stage size-segregated aerosol samples collected from Cizao Town, Jinjiang City, Fujian Province, China, in April 2009. The regression lines are forced through the origin. In Figure 12a, two outlier points deviating from the linear regression line are indicated as solid circles and are excluded from the regression.

source of carbonaceous aerosols, whereas biomass burning could have been a possible source. As mentioned above, Jinjiang City is a very important manufacturing area of sport shoes and jackets. Chemicals used in shoemaking, particularly the solvents, have been demonstrated to be a significant source of ambient VOCs in the PRD [*Chan et al.*, 2006]. Accordingly, secondary organic aerosols may form through the oxidation of VOCs and gas-to-particle conversion of the resulting reaction products [*Xiao et al.*, 2009]. Thus oxidation products of VOCs emitted from Jinjiang City might have been one of the principal contributors to OC observed in Kinmen.

[39] Nonetheless, the measured mean OC/EC ratio cannot be used to precisely differentiate between secondary organic aerosols and organic aerosol species derived from biomass burning, as they may have similar OC/EC ratios [*Sillanpää et al.*, 2005; *Tan et al.*, 2009]. Also note that OC/EC ratios are site specific. In order to assess the contribution of biomass burning, we further examined the relationship between OC and non-sea-salt K^+, showing a slope of 7.5 with a moderate correlation (R = 0.53; Figure 13b). This seems to suggest that biomass burning could also be a possible source of OC in Kinmen aerosols [*Duan et al.*, 2004], which is reasonable, as biomass fuels are commonly used in rural parts of China during the winter months for heating and cooking. On the other hand, the contribution of secondary organic species to the ambient OC currently cannot be precisely determined and thus merits more investigations in the future.

4.7. Implications for Regional Pollution, Atmospheric Chemistry, and Climate

[40] The combined evaluation of air-quality data and aerosol chemical composition demonstrates that Kinmen is impacted by substantial air pollution associated with industrial operations in areas to the north along the coast of Fujian Province, especially during the northeastern monsoon. Our finding also clearly suggest that PM sources are numerous and of mixed nature, which has important implications for atmospheric chemistry of aerosol particles in terms of their physicochemical properties, mixing states (internally versus

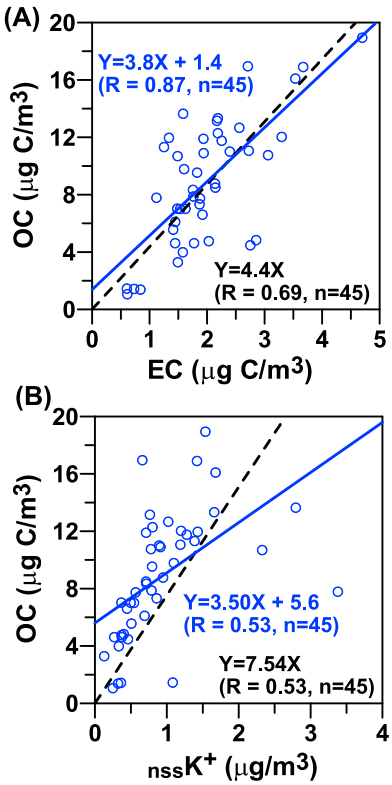

Figure 13. Scatterplots of (a) OC and EC in TSP aerosol filter samples and (b) OC measured in the TSP and non-sea-salt K^+ measured in the PM_{10} aerosol filter samples collected on Kinmen Island. Linear regressions were computed for each plot by forcing and not forcing the line through the origin.

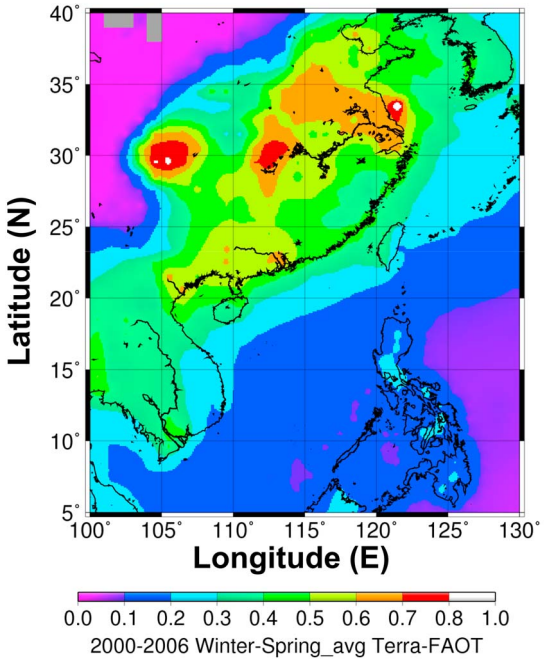

Figure 14. Spatial distribution of the Fine mode Aerosol Optical Thickness observation from the NASA/Terra MODIS sensor over the western Pacific Ocean in the prevailing northeasterly monsoon seasons (i.e., winter and spring) averaged between 2000 and 2006.

externally mixed), and gas-particle interactions, thus influencing radiative forcing and human health [*Shao et al.*, 2006]. Certain anthropogenic activities, including ceramic/pottery manufacturing as well as shoe-making and textile industries in Jinjiang City, Fujian Province, were shown to likely be the chief air pollution sources for Kinmen Island. Aside from traditional anthropogenic emission sources, such as fossil fuel combustion, traffic exhausts, biomass burning, and fugitive road dust, these abovementioned sources may have significant contributions to PM pollution in China as well, because many industrial cities like Jinjiang City, with mixed emission sources, are prevalent and distributed widely throughout China, while their influences on regional air quality has largely been overlooked.

[41] More importantly, while most studies addressing air pollution in China have been focused on the YRD and the PRD regions, our study shows that areas in-between (e.g., Fujian Province) these two urban and industrial hubs suffer from severe air pollution as well. Remote sensing observations, such as the Fine mode Aerosol Optical Thickness (FAOT) from NASA's Terra MODerate Resolution Imaging Spectro-radiometer (MODIS) sensor (Figure 14) [*Kaufman et al.*, 2002; *Remer et al.*, 2005; *Lin et al.*, 2007, 2009], confirm our conclusion. As shown in Figure 14, the spatial distribution of FAOT data reveals that fine aerosol pollution may extend from the YRD toward the PRD regions, forming a tongue-like, regional pollution zone, which is also consistent with the distribution of tropospheric NO_2 in eastern China [*Zhang et al.*, 2007]. Aside from their adverse impacts on human health, mixed aerosol particles could also pose complex effects on climate forcing on a regional scale [*Qian et al.*, 2009]. Therefore, such middle- to large-scale pollution phenomena, particularly in China, warrant further scientific, as well as regulatory, attention.

5. Summary

[42] Based on our results, we can draw the following conclusions:

[43] 1. Air-quality data measured on the offshore island, Kinmen, between 2004 and 2008 reveal consistently high PM concentrations during the study period, particularly in winter. Highest values were achieved in the last two years (i.e., 2007 and 2008).

[44] 2. Abnormally high PM concentrations preferentially occurred in the early morning and are essentially due to ineffective dispersion because of low wind speeds and lower mixed heights, leading to the accumulation of primary aerosols and likely the formation of secondary aerosols, which merits more investigations in the future.

[45] 3. The principal components of aerosol particles were sulfate, mineral dust, and POM. Other minor components include nitrate, ammonium, sea salt, EC, and heavy metal oxides. Unidentified components accounted for 18% of the total aerosol mass.

[46] 4. Clay mineral dust and reactive gas (e.g., SO_2) emissions from ceramic industries in the northern part of Fujian Province's coastal area, specifically Jinjiang City, likely constituted the key components of the observed aerosol pollution in Kinmen. An additional crucial PM source were organic aerosols, likely resulting from biomass/biofuel burning activities in rural areas of Fujian Province as well as oxidation of VOCs presumably emitted from petrochemical sources and solvents used in shoemaking factories, warranting future investigations.

[47] 5. The numerous and mixed sources of Kinmen ambient aerosols result in critical implications for atmospheric chemistry, e.g., in terms of aerosol mixing state and gas-particle interactions. Furthermore, these aerosols are likely involved in complex climate forcing processes. Combining our findings with satellite images, we clearly show the large-scale extent of aerosol pollution along the coastal lines of Eastern China, extending from the YRD to the PRD, and thus imposing significant regional-scale effects on air quality, biogeochemical cycles, and climate.

[48] **Acknowledgments.** The authors are grateful to three anonymous reviewers for their constructive comments. We thank the Environmental Protection Administration of ROC for providing us with air-quality data. We appreciate Jinning Elementary and Junior High School for generously providing the aerosol sampling location. Thanks are also due to the NASA MODIS team for providing the remote sensing data. We also thank the NOAA Air Resources Laboratory (ARL) for the provision of the HYSPLIT transport and dispersion model and/or READY web site (http://www.arl.noaa.gov/ready.html) used in this study. This work was supported by the National Science Council (NSC) of Taiwan (grant NSC 97-2111-M-001-001-MY2), and in part by the thematic program, Atmospheric Forcing on Ocean Biogeochemistry (AFOBi), of Academia Sinica. We also thank the Center for Marine Bioscience and Biotechnology, NTOU, for their support to S.C.H.

References

Ando, M., et al. (2001), Health effects of fluoride pollution caused by coal burning, *Sci. Total Environ.*, *271*, 107–116, doi:10.1016/S0048-9697(00)00836-6.

Andreae, M. O., and P. J. Crutzen (1997), Atmospheric aerosols: Biogeochemical sources and role in atmospheric chemistry, *Science*, *276*, 1052–1058, doi:10.1126/science.276.5315.1052.

Andreae, M. O., O. Schmida, H. Yang, D. Chanda, J. Z. Yu, L. M. Zeng, and Y. H. Zhang (2008), Optical properties and chemical composition of the atmospheric aerosol in urban Guangzhou, *China, Atmos. Environ.*, *42*, 6335–6350, doi:10.1016/j.atmosenv.2008.01.030.

Bi, X., Y. Feng, J. Wu, Y. Wang, and T. Zhu (2007), Source apportionment of PM_{10} in six cities of northern China, *Atmos. Environ.*, *41*, 903–912, doi:10.1016/j.atmosenv.2006.09.033.

Brock, C. A., et al. (2008), Sources of particulate matter in the northeastern United States in summer: 2. Evolution of chemical and microphysical properties, *J. Geophys. Res.*, *113*, D08302, doi:10.1029/2007JD009241.

Brook, J. R., T. F. Dann, and R. T. Burnett (1997), The relationship among TSP, PM_{10}, $PM_{2.5}$ and inorganic constituents of atmospheric particulate matter at multiple Canadian locations, *J. Air Waste Manage. Assoc.*, *47*, 2–19.

Cao, J. J., et al. (2007), Spatial and seasonal distributions of carbonaceous aerosols over China, *J. Geophys. Res.*, *112*, D22S11, doi:10.1029/2006JD008205.

Cao, J., Z. Shen, J. C. Chow, G. Qi, and J. G. Watson (2009), Seasonal variations and sources of mass and chemical composition for PM_{10} aerosol in Hangzhou, China, *Particuology*, *7*, 161–168, doi:10.1016/j.partic.2009.01.009.

Cass, G. R., L. A. Hughes, P. Bhave, M. J. Kleeman, J. O. Allen, and L. G. Salmon (2000), The chemical composition of atmospheric ultrafine particles, *Philos. Trans. R. Soc. London, Ser. A*, *358*, 2581–2592, doi:10.1098/rsta.2000.0670.

Chan, C. K., and X. Yao (2008), Air pollution in mega cities in China, *Atmos. Environ.*, *42*, 1–42, doi:10.1016/j.atmosenv.2007.09.003.

Chan, L. Y., K. W. Chu, S. C. Zou, C. Y. Chan, X. M. Wang, B. Barletta, D. R. Blake, H. Guo, and W. Y. Tsai (2006), Characteristics of nonmethane hydrocarbons (NMHCs) in industrial, industrial-urban, and industrial-suburban atmospheres of the Pearl River Delta (PRD) region of south China, *J. Geophys. Res.*, *111*, D11304, doi:10.1029/2005JD006481.

Charlson, R. J., S. E. Schwartz, J. M. Hales, R. D. Cess, J. A. Coakley Jr., J. E. Hansen, and D. J. Hofmann (1992), Climate forcing by anthropogenic aerosols, *Science*, *255*, 423–430, doi:10.1126/science.255.5043.423.

Chester, R., M. Nimmo, G. R. Fones, S. Keyse, and Z. Zhang (2000), Trace metal chemistry of particulate aerosols from the UK mainland coastal rim of the NE Irish Sea, *Atmos. Environ.*, *34*, 949–958, doi:10.1016/S1352-2310(99)00234-4.

Chou, C. C. K., S. H. Huang, T. K. Chen, C. Y. Lin, and L. C. Wang (2005), Size-segregated characterization of atmospheric aerosols in Taipei during Asian outflow episodes, *Atmos. Res.*, *75*, 89–109, doi:10.1016/j.atmosres.2004.12.002.

Chow, J. C., and J. G. Watson (2002), $PM_{2.5}$ carbonate concentrations at regionally representative Interagency Monitoring of Protected Visual Environment sites, *J. Geophys. Res.*, *107*(D21), 8344, doi:10.1029/2001JD000574.

Chow, J. C., J. G. Watson, Z. Lu, D. H. Lowenthal, C. A. Frazier, P. A. Solomon, and R. H. Thuillier (1996), Descriptive analysis of $PM_{2.5}$ and PM_{10} at regionally representative locations during SJVAQS/AUSPEX, *Atmos. Environ.*, *30*, 2079–2112, doi:10.1016/1352-2310(95)00402-5.

Chu, D. A., Y. J. Kaufman, G. Zibordi, J. D. Chern, J. Mao, C. Li, and B. N. Holben (2003), Global monitoring of air pollution over land from the Earth Observing System-Terra Moderate Resolution Imaging Spectroradiometer (MODIS), *J. Geophys. Res.*, *108*(D21), 4661, doi:10.1029/2002JD003179.

Cooper, D. J., A. J. Watson, and P. D. Nightingale (1996), Large decrease in ocean-surface CO_2 fugacity in response to in situ iron fertilization, *Nature*, *383*, 511–513, doi:10.1038/383511a0.

Duan, F., X. Liu, T. Yu, and H. Cachier (2004), Identification and estimate of biomass burning contribution to the urban aerosol organic carbon concentrations in Beijing, *Atmos. Environ.*, *38*, 1275–1282, doi:10.1016/j.atmosenv.2003.11.037.

Edgerton, E. S., B. E. Hartsell, R. D. Saylor, J. J. Jansen, D. A. Hansen, and G. M. Hidy (2005), The Southeastern Aerosol Research and Characterization Study: Part II. Filter-based measurements of fine and coarse particulate matter mass and composition, *J. Air Waste Manage. Assoc.*, *55*, 1527–1542.

Fang, G. C., Y. S. Wu, T. Y. Chou, and C. Z. Lee (2008), Organic carbon and elemental carbon in Asia: A review from 1996 to 2006, *J. Hazard. Mater.*, *150*, 231–237, doi:10.1016/j.jhazmat.2007.09.036.

Fang, M., C. K. Chan, and X. Yao (2009), Managing air quality in a rapidly developing nation: China, *Atmos. Environ.*, *43*, 79–86, doi:10.1016/j.atmosenv.2008.09.064.

Finkelman, R. B., H. E. Belkin, and B. Zheng (1999), Health impacts of domestic coal use in China, *Proc. Natl. Acad. Sci. U. S. A.*, *96*, 3427–3431, doi:10.1073/pnas.96.7.3427.

Guo, J. P., et al. (2009), Correlation between PM concentrations and aerosol optical depth in eastern China, *Atmos. Environ.*, *43*, 5876–5886, doi:10.1016/j.atmosenv.2009.08.026.

Ho, K. F., S. C. Lee, C. K. Chan, J. C. Yu, J. C. Chow, and X. H. Yao (2003), Characterization of chemical species in $PM_{2.5}$ and PM_{10} aerosols in Hong Kong, *Atmos. Environ.*, *37*, 31–39, doi:10.1016/S1352-2310(02)00804-X.

Hong, H. S., H. L. Yin, X. H. Wang, and C. X. Ye (2007), Seasonal variation of PM_{10}-bound PAHs in the atmosphere of Xiamen, China, *Atmos. Res.*, *85*, 429–441, doi:10.1016/j.atmosres.2007.03.004.

Hsu, S. C., S. C. Liu, S. J. Kao, W. L. Jeng, Y. T. Huang, C. M. Tseng, F. Tsai, J. Y. Tu, and Y. Yang (2007), Water soluble species in the marine aerosol from the northern South China Sea: High chloride depletion related to air pollution, *J. Geophys. Res.*, *112*, D19304, doi:10.1029/2007JD008844.

Hsu, S. C., S. C. Liu, Y. T. Huang, S. C. C. Lung, F. Tsai, J. Y. Tu, and S. J. Kao (2008), A criterion for identifying Asian dust events based on Al concentration data collected from northern Taiwan between 2002 and early 2007, *J. Geophys. Res.*, *113*, D18306, doi:10.1029/2007JD009574.

Hsu, S. C., S. C. Liu, Y. T. Huang, C. C. K. Chou, S. C. C. Lung, T. H. Liu, J. Y. Tu, and F. Tsai (2009a), Long-range southeastward transport of Asian biosmoke pollution: Signature detected by aerosol potassium in northern Taiwan, *J. Geophys. Res.*, *114*, D14301, doi:10.1029/2009JD011725.

Hsu, S. C., S. C. Liu, R. Arimoto, T. H. Liu, Y. T. Huang, F. Tsai, F. J. Lin, and S. J. Kao (2009b), Dust deposition to northern Taiwan and its biogeochemical implications in the East China Sea, *J. Geophys. Res.*, *114*, D15304, doi:10.1029/2008JD011223.

Hueglin, C., R. Gehrig, U. Baltensperger, M. Gysel, C. Monn, and H. Vonmont (2005), Chemical characterisation of $PM_{2.5}$, PM_{10} and coarse particles at urban, near-city and rural sites in Switzerland, *Atmos. Environ.*, *39*, 637–651, doi:10.1016/j.atmosenv.2004.10.027.

Intergovernmental Panel on Climate Change (2001), Climate Change 2001, *Contribution of Working Group I to the Third Assessment Report of the Intergovernmental Panel on Climate Change*, 881 pp., Cambridge Univ. Press, New York.

Junker, C., J. L. Wang, and C. T. Lee (2009), Evaluation of the effect of long-range transport of air pollutants on coastal atmospheric monitoring sites in and around Taiwan, *Atmos. Environ.*, *43*, 3374–3384, doi:10.1016/j.atmosenv.2009.03.035.

Kahnert, M., T. Nousiainen, and B. Veihelmann (2005), Spherical and spheroidal model particles as an error source in aerosol climate forcing and radiance computations: A case study for feldspar aerosols, *J. Geophys. Res.*, *110*, D18S13, doi:10.1029/2004JD005558.

Kaufman, Y. J., D. Tanré, and O. Boucher (2002), A satellite view of aerosols in the climate system, *Nature*, *419*, 215–223, doi:10.1038/nature01091.

Koulouri, E., S. Saarikoski, C. Theodosi, Z. Markaki, E. Gerasopoulos, G. Kouvarakis, T. Mäkela, R. Hillamo, and N. Mihalopoulos (2008), Chemical composition and sources of fine and coarse aerosol particles in the Eastern Mediterranean, *Atmos. Environ.*, *42*, 6542–6550, doi:10.1016/j.atmosenv.2008.04.010.

Krishnan, P., and P. K. Kunhikrishnan (2004), Temporal variations of ventilation coefficient at a tropical Indian station using UHF wind profiler, *Curr. Sci.*, *86*, 447–451.

Landis, M. S., G. A. Norris, R. W. Williams, and J. P. Weinstein (2001), Personal exposures to $PM_{2.5}$ mass and trace elements in Baltimore, MD, USA, *Atmos. Environ.*, *35*, 6511–6524, doi:10.1016/S1352-2310(01)00407-1.

Lee, C. T., and W. C. Hsu (1998), A novel method to measure aerosol water mass, *J. Aerosol Sci.*, *29*, 827–837, doi:10.1016/S0021-8502(97)00434-5.

Lin, I. I., J. P. Chen, G. T. F. Wong, C.-W. Huang, and C.-C. Lien (2007), Aerosol input to the South China Sea: Results from the moderate resolution imaging spectro-radiometer, the quick scatterometer, and the measurements of pollution in the troposphere sensor, *Deep Sea Res., Part II*, *54*, 1589–1601, doi:10.1016/j.dsr2.2007.05.013.

Lin, I. I., G. T. F. Wong, C.-C. Lien, C.-Y. Chien, C.-W. Huang, and J.-P. Chen (2009), Aerosol impact on the South China Sea biogeochemistry: An early assessment from remote sensing, *Geophys. Res. Lett.*, *36*, L17605, doi:10.1029/2009GL037484.

Lingard, J. J. N., A. S. Tomlin, A. G. Clarke, K. Healey, A. W. M. Hay, C. P. Wild, and M. N. Routledge (2005), A study of trace metal concentration of urban airborne particulate matter and its role in free radical activity as measured by plasmid strand break assay, *Atmos. Environ.*, *39*, 2377–2384, doi:10.1016/j.atmosenv.2004.05.063.

Malm, W. C., J. F. Sisler, D. Huffman, R. A. Eldred, and T. A. Cahill (1994), Spatial and seasonal trends in particle concentration and optical

extinction in the United States, *J. Geophys. Res.*, *99*, 1347–1370, doi:10.1029/93JD02916.

Malm, W. C., B. A. Schichtel, M. L. Pitchford, L. L. Ashbaugh, and R. A. Eldred (2004), Spatial and monthly trends in speciated fine particle concentration in the United States, *J. Geophys. Res.*, *109*, D03306, doi:10.1029/2003JD003739.

Martin, J. H., et al. (1994), Testing the iron hypothesis in ecosystems of the equatorial Pacific Ocean, *Nature*, *371*, 123–129, doi:10.1038/371123a0.

Ondov, J. M., T. J. Buckley, P. K. Hopke, D. Ogulei, M. B. Parlange, W. F. Rogge, K. S. Squibb, M. V. Johnston, and A. S. Wexler (2006), Baltimore supersite: Highly time- and size-resolved concentrations of urban $PM_{2.5}$ and its constituents for resolution of sources and immune responses, *Atmos. Environ.*, *40*, Suppl. 2, 224–237, doi:10.1016/j.atmosenv.2005.11.072.

Prather, K. A., C. D. Hatch, and V. H. Grassian (2008), Analysis of atmospheric aerosols, *Annu. Rev. Anal. Chem.*, *1*, 485–514, doi:10.1146/annurev.anchem.1.031207.113030.

Qian, Y., D. Gong, J. Fan, L. R. Leung, R. Bennartz, D. Chen, and W. Wang (2009), Heavy pollution suppresses light rain in China: Observations and modeling, *J. Geophys. Res.*, *114*, D00K02, doi:10.1029/2008JD011575.

Querol, X., et al. (2007), Source origin of trace elements in PM from regional background, urban and industrial sites of Spain, *Atmos. Environ.*, *41*, 7219–7231, doi:10.1016/j.atmosenv.2007.05.022.

Remer, L. A., et al. (2005), The MODIS aerosol algorithm, products and validation, *J. Atmos. Sci.*, *62*, 947–973, doi:10.1175/JAS3385.1.

Ryu, S. Y., J. E. Kim, H. Zhuanshi, and Y. J. Kim (2004), Chemical composition of post-harvest biomass burning aerosols in Gwangju, Korea, *J. Air Waste Manage. Assoc.*, *54*, 1124–1137.

Sciare, J., H. Bardouki, C. Moulin, and N. Mihalopoulos (2003), Aerosol sources and their contribution to the chemical composition of aerosols in the eastern Mediterranean Sea during summertime, *Atmos. Chem. Phys.*, *3*, 291–302, doi:10.5194/acp-3-291-2003.

Seinfeld, J. H. (1989), Urban air pollution: State of the science, *Science*, *243*, 745–752, doi:10.1126/science.243.4892.745.

Seinfeld, J. (2008), Black carbon and brown clouds, *Nat. Geosci.*, *1*, 15–16, doi:10.1038/ngeo.2007.62.

Seinfeld, J. H., and S. N. Pandis (1998), *Atmospheric Chemistry and Physics: From Air Pollution to Climate Change*, 1326 pp., John Wiley, Hoboken, N. J.

Shao, M., X. Y. Tang, Y. H. Zhang, and W. Li (2006), City clusters in China: Air and surface water pollution, *Front. Ecol. Environ.*, *4*, 353–361, doi:10.1890/1540-9295(2006)004[0353:CCICAA]2.0.CO;2.

Sillanpää, M., A. Frey, R. Hillamo, A. S. Pennanen, and R. O. Salonen (2005), Organic, elemental and inorganic carbon in particulate matter of six urban environments in Europe, *Atmos. Chem. Phys.*, *5*, 2869–2879, doi:10.5194/acp-5-2869-2005.

Tan, J. H., J. C. Duan, D. H. Chen, X. H. Wang, S. J. Guo, X. H. Bi, G. Y. Sheng, K. B. He, and J. M. Fu (2009), Chemical characteristics of haze during summer and winter in Guangzhou,*Atmos. Res.*, *94*, 238–245, doi:10.1016/j.atmosres.2009.05.016.

Taylor, S. R. (1964), Abundance of chemical elements in the continental crust: A new table, *Geochim. Cosmochim. Acta*, *28*, 1273–1285, doi:10.1016/0016-7037(64)90129-2.

Tegen, I., A. A. Lacis, and I. Fung (1996), The influence on climate forcing of mineral aerosols from disturbed soils, *Nature*, *380*, 419–422, doi:10.1038/380419a0.

Turpin, B. J., and H. J. Lim (2001), Species contributions to $PM_{2.5}$ mass concentrations: Revisiting common assumptions for estimating organic mass, *Aerosol Sci. Technol.*, *35*, 602–610, doi:10.1080/02786820152051454.

Turpin, B. J., R. A. Cary, and J. J. Huntzicker (1990), Identification of secondary organic aerosol episodes and quantification of primary and secondary organic aerosol concentrations during SCAQS, *Aerosol Sci. Technol.*, *12*, 161–171, doi:10.1080/02786829008959336.

Viidanoja, J., M. Sillanpää, J. Laakia, V. M. Kerminen, R. Hillamo, P. Aarnio, and T. Koskentalo (2002), Organic and black carbon in $PM_{2.5}$ and PM_{10}: 1 year of data from an urban site in Helsinki, Finland, *Atmos. Environ.*, *36*, 3183–3193, doi:10.1016/S1352-2310(02)00205-4.

Wang, X. H., C. X. Ye, H. L. Yin, M. Z. Zhuang, S. P. Wu, J. L. Mu, and H. S. Hong (2007), Contamination of polycyclic aromatic hydrocarbons bound to PM_{10}/$PM_{2.5}$ in Xiamen, China, *Aerosol Air Qual. Res.*, *7*, 260–276.

Watson, J. G., J. C. Chow, D. H. Lowenthal, L. C. Pritchett, C. A. Frazier, G. R. Neuroth, and R. Robbins (1994), Differences in the carbon composition of source profiles for diesel- and gasoline-powered vehicles, *Atmos. Environ.*, *28*, 2493–2505, doi:10.1016/1352-2310(94)90400-6.

Wei, Y., I. K. Han, M. Shao, M. Hu, J. J. Zhang, and X. Tang (2009), $PM_{2.5}$ constituents and oxidative DNA damage in humans, *Environ. Sci. Technol.*, *43*, 4757–4762, doi:10.1021/es803337c.

Xiao, R., et al. (2009), Formation of submicron sulfate and organic aerosols in the outflow from the urban region of the Pearl River Delta in China, *Atmos. Environ.*, *43*, 3754–3763, doi:10.1016/j.atmosenv.2009.04.028.

Xu, M., R. Yan, C. Zheng, Y. Qiao, J. Han, and C. Sheng (2004), Status of trace element emission in a coal combustion process: A review, *Fuel Process. Technol.*, *85*, 215–237, doi:10.1016/S0378-3820(03)00174-7.

Yauk, C., et al. (2008), Germ-line mutations, DNA damage, and global hypermethylation in mice exposed to particulate air pollution in an urban/industrial location, *Proc. Natl. Acad. Sci. U. S. A.*, *105*, 605–610, doi:10.1073/pnas.0705896105.

Yuan, Z., A. K. H. Lau, H. Zhang, J. Z. Yu, P. K. K. Louie, and J. C. H. Fung (2006), Identification and spatiotemporal variations of dominant PM_{10} sources over Hong Kong, *Atmos. Environ.*, *40*, 1803–1815, doi:10.1016/j.atmosenv.2005.11.030.

Zhang, X. Y., R. Arimoto, and Z. S. An (1997), Dust emission from Chinese desert sources linked to variations in atmospheric circulation, *J. Geophys. Res.*, *102*, 28,041–28,047, doi:10.1029/97JD02300.

Zhang, X. Y., S. L. Gong, R. Arimoto, Z. X. Shen, F. M. Mei, D. Wang, and Y. Cheng (2003), Characterization and temporal variation of Asian dust aerosol from a site in the northern Chinese deserts, *J. Atmos. Chem.*, *44*, 241–257, doi:10.1023/A:1022900220357.

Zhang, X. Y., P. Zhang, Y. Zhang, X. J. Li, and H. Qiu (2007), The trend, seasonal cycle, and sources of tropospheric NO_2 over China during 1997−2006 based on satellite measurement, *Sci. China, Ser. D*, *50*, 1877–1884.

C. Y. Chan, School of Environmental Science and Engineering, Sun Yat-Sen University, 135 Xingang West Rd., Guangzhou 510275, China.

W. N. Chen, K. H. Chi, C. K. C. Chou, G. Engling, S. C. Hsu (corresponding author), C. H. Huang, Y. T. Huang, S. J. Kao, C. L. Kuo, S. C. Liu, S. C. C. Lung, and T. C. Wu, Research Center for Environmental Changes, Academia Sinica, PO Box 1-48, Nanking, Taipei 11529, Taiwan. (schsu815@rcec.sinica.edu.tw)

J. C. Huang, Department of Geography, National Taiwan University, No. 1, Sec. 4, Roosevelt Road, Taipei 10617, Taiwan.

F. J. Lin, Institute of Oceanography, National Taiwan University, No. 1, Sec. 4, Roosevelt Road, Taipei 10617, Taiwan.

I. I. Lin, Department of Atmospheric Science, National Taiwan University, No. 1, Sec. 4, Roosevelt Road, Taipei 10617, Taiwan.

S. C. Lin, Department of Construction Engineering, National Quemoy University, University Road, Jinning Township, Kinmen 892, Taiwan.

F. Tsai, Department of Marine Environmental Informatics, National Taiwan Ocean University, No. 2, Pei-Ning Road, Keelung 20224, Taiwan.